

Author's response on the revised manuscript "Impact of reactive surfaces on the abiotic reaction between nitrite and ferrous iron and associated nitrogen and oxygen isotope dynamics" by Anna-Neva Visser et al.

1. Point-by-Point response to the reviews

1.1. Response to comments by Anonymous Referee #1

First, we wish to thank the reviewer for his/her valuable inputs and comments on our manuscript.

L39-40: I'm surprised there are no older references to the role of iron.

Reply: We agree that indeed there are many more references regarding the role of iron in the environment. However, our choice can be considered as "best of" selection, covering a whole suite of different aspects: we choose (1) Expert et al., 2012 since they explicitly focus on the vital role of iron for all living organisms, its wide range of redox potentials and its catalytic role in various metabolic pathways; (2) Lovley et al., 1997, who reported on the importance of iron already in 1988, however, the publication chosen represents a nice "summary", focusing also on various reactions and thus its "remediative" capabilities. Obviously, we wanted to limit the number of references, but if the reviewer thinks of a specific publication, we will be happy to include it. Again, in light of the many publications on the importance of iron available, and since our manuscript is already very long, we simply decided to pick two references that support the statement/sentence.

General experiment setup section: The conditions of the experiment are anoxia and the addition of iron and nitrogen in the form of nitrite. Under these conditions, in the environment, it is conceivable that dissimilative reduction of nitrite to ammonium may occur. Of course under perfect abiotic conditions DNRA should not occur. Did the authors measure ammonium concentrations throughout the experiment to ensure that no other processes than the one under study were taking place?

Reply: As the reviewer stated, DNRA should not occur under abiotic conditions. Considering that the abiotic experiments were all performed under laboratory conditions, using a medium that contains already high amounts of ammonium (5.61 mM NH_4Cl , see 2.1), ammonium concentrations were only checked sporadically for some setups. Since only (if at all) minor fluctuations were observed, no further efforts to determine ammonium concentrations were attempted.

L120-121: How long does it take from incubation to the measurement of concentrations and isotopes? Light is a factor that can generate abiotic reactions, which in turn can generate isotope fractionation. What about it?

Reply: Yes, light-induced reactions have to be considered. That was one reason why nitrite concentrations were measured via CFA immediately after the samples were taken (within one hour). After determining the nitrite concentrations, the azide method was applied (within max. 2-3 hrs). Samples were kept inside the glovebox in coloured (dark brown or blue) Eppendorf tubes, whereas the latter were chosen to inhibit potential photocatalytic reactions. The azide-treated headspace vials were stored in card boxes at RT until measured. At this point, the sample is fixed (i.e., turned into N_2O). Therefore, we are rather confident that neither light nor (possibly) temperature could have influenced the values. However, one could argue that the blue coloured Eppendorf tubes might not suffice, since they are indeed partly translucent. Since during one of the experiments blue and brown vials were used, and still, the concentration values within the nine replicates were very similar (see Figure 1 A and C,

note error bars), we are confident that the rapid processing and precautions taken to avoid light-induced reactions did indeed suffice.

L179-180: Two nitrite isotope standards have been used. What are the values of these standards? Do these values include those of the samples measured in this study? What is the analytical precision of the method (preparation + intrinsic analysis) for the determination of the isotopic composition of nitrite (15N and 18O)?

Reply: Standard N-7373 has a $\delta^{15}\text{N}$ value of -79.6‰ and a $\delta^{18}\text{O}$ value of +4.5‰. In contrast, standard N-10219 has a $\delta^{15}\text{N}$ value of +2.8‰ and a $\delta^{18}\text{O}$ value of +88.5‰. Using both standards allowed for the reliable correction using standard bracketing: The standard $\delta^{15}\text{N}$ range included the $\delta^{15}\text{N}$ values obtained for our samples perfectly. The $\delta^{18}\text{O}$ values measured fell only slightly below (-0.5 to 2.5‰) the range given by the standards, so that corrections are reliable. Based on replicate measurements of laboratory standards and samples, the analytical precision for NO_2^- $\delta^{15}\text{N}$ and $\delta^{18}\text{O}$ analyses was $\pm 0.4\%$ and $\pm 0.6\%$ (1 SD), respectively.

L285-291: Rayleigh conditions allow the isotope fractionation factor to be easily determined by looking at the slope of the line on a representation $\ln C/C_0$ as a function of $\delta^{15}\text{N}$, but not C (with C the concentration at time t and C_0 the initial concentration). This paragraph is not clear to me. Moreover, doesn't the fact that there is first a decrease of ^{15}N , i.e. an inverse isotopic fractionation, with a decrease of the amount of heavy isotope in the residual substrate, and then an enrichment, mean that several processes could take place and that process 1 takes place at the beginning of the experiment with a higher rate than the second process which either starts at the beginning of the experiment or when process 1 is completed? Very concretely, the trend line is calculated on the points starting from the lowest $\delta^{15}\text{N}$ values? I think it would be necessary to clarify this part.

Reply: We agree, the title of the x-axis of Figure 5 might be misleading. Of course, the values of the x-axis represent the \ln of the substrate fraction remaining (as mentioned in the caption below the figure). Hence, it is the $\ln(f)$ whereas f is C/C_0 . We will change the title of the x-axis to avoid future confusions. With regards to the second comment, i.e., that the data presented might simply reflect that two different processes are at work, we also agree. However, since it is hard to explain which processes might be at work and if this is indeed a clear inverse effect, we decided to calculate the isotope effect using the lowest $\delta^{15}\text{N}$ values observed (i.e. for the experimental period where we show a clear decline in nitrite concentration with a net increase in $\delta^{15}\text{N}$). We will clarify that there is putative evidence for multiple processes occurring in the incubations, and that this has implications for the Rayleigh approach.

L296-302: Is it not possible to envisage that the variations in ^{18}O are due solely to an exchange between the oxygen of the nitrite and the oxygen of the water? By the way, what is the isotopic composition of water? Is it constant during the experiment?

Reply: Unfortunately, the isotopic composition of the water was not measured, and we can only assume its $\delta^{18}\text{O}$ (the water used in Tübingen has a $\delta^{18}\text{O}$ of roughly 11‰). It is possible that the variations in $\delta^{18}\text{O}$ are partially attributable to oxygen atom exchange dynamics with the matrix (see e.g. L504-516). However, considering that the observed drop in $\delta^{18}\text{O}$ values in both experiments occurs more or less simultaneously with the drop in $\delta^{15}\text{N}$ might be indicative of other dynamics (e.g. sorption, complexation?).

L309-313: The authors have done a significant analytical work. Why not show the variations in N_2O concentration as a function of nitrite concentrations? Before any interpretation with isotopes or isotopologists, it seems to me useful and necessary to work on the concentrations and in particular to make mass balances.

Reply: The proposed graph could be added to the supplementary material. However, particularly for the mineral only setups, this way of visualizing the data does not help much (see graph added). Also, for the main manuscript we had severe concerns with regards to its length. Therefore, we chose to present only

graphs that really help to understand the main messages of this project. With regards to the mass balance: The initial objectives of this project included mass balance considerations since it was supposed to lay the ground for a following study on nitrate-dependent Fe(II) oxidation in selected microbial strains. Unfortunately, we did not have the capacities to also analyse the N_2 samples, so a proper mass balance is unfortunately not possible.

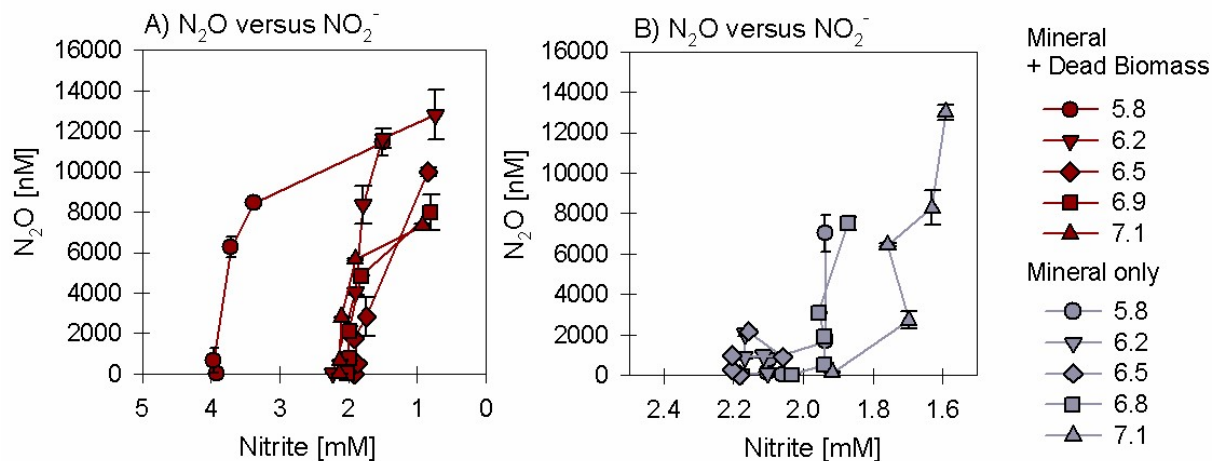


Figure 1: N_2O vs NO_2^- concentrations in (A) mineral plus dead biomass and (B) mineral only experiment

L314-315: The authors do not discuss the very negative SP value, which is very distinct from the other points. Is this an analytical problem?

Reply: We assume that the reviewer is referring to the observed drops in SP values (-120 to -80‰), occurring at t_1 for samples taken from the mineral + dead biomass setup at pH 6.2 and mineral only at pH 5.8. After another thorough check of the raw data, we have to admit that for those particular samples the peak areas of the data obtained via CF-IRMS were much higher (compared to standards), possibly causing an extreme linearity or contamination effect that is affecting the data. We re-checked the entire data set again and removed these outliers (see revised figure below). The bulk of the data is not compromised, as we have good agreement between the standard and the sample peak areas.

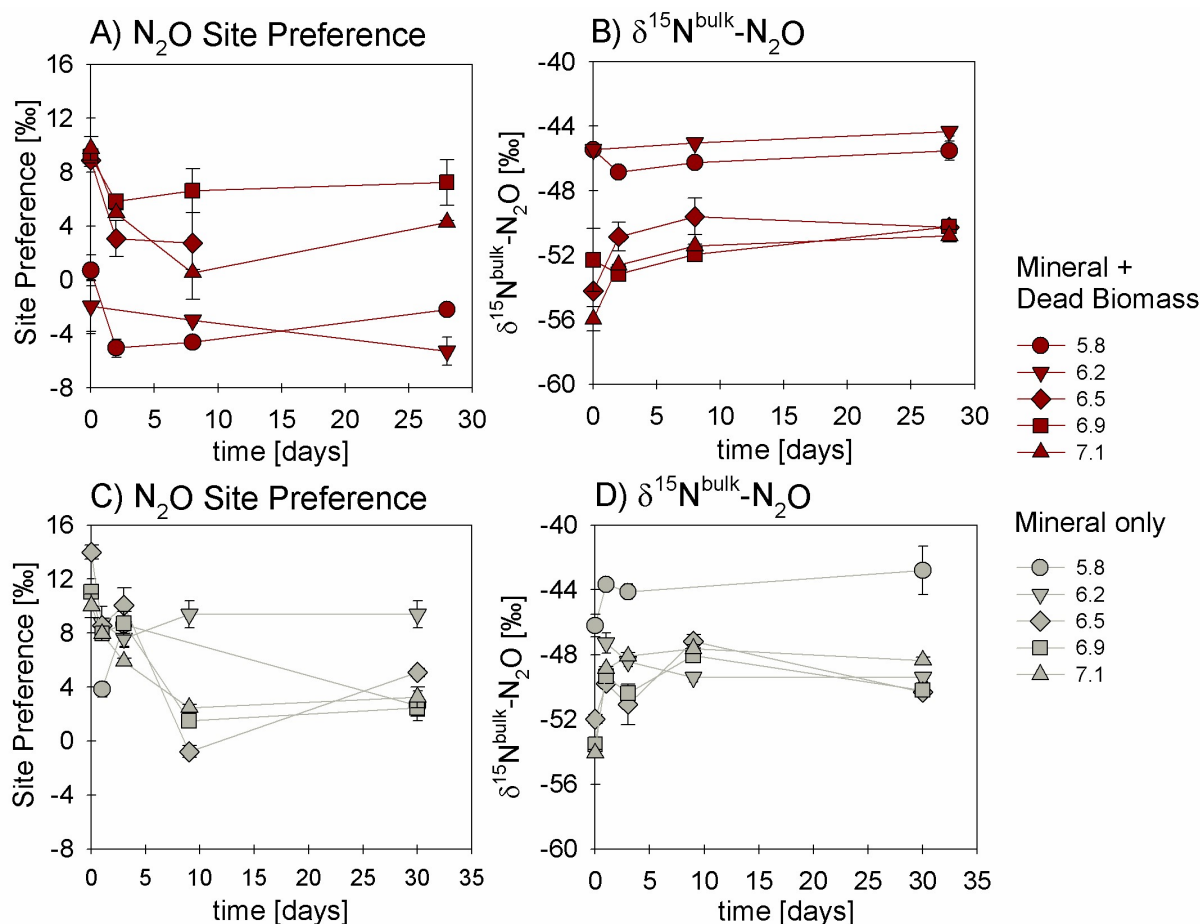


Figure 2: Site Preference (SP; A, C) and $\delta^{15}\text{N}^{\text{bulk}}-\text{N}_2\text{O}$ (B, D) values of N_2O produced in experiments amended with mineral + dead biomass (red) and mineral-only (grey)

L326: There is no figure S6. But mentioned in S5 section figure 3.

Reply: We thank the reviewer for pointing this out and apologize for the mistake. Figure S5 mentioned in L322 actually corresponds to Figure S4 in the supplements, while S6 in L 326 refers to S5! We will change this in the re-submitted version of the MS.

L484-486: Large variations of $\delta^{15}\text{N}$ are not associated with variations of $\delta^{18}\text{O}$. While these are measurements made on the residual substrate. The drop in $\delta^{18}\text{O}$ at the beginning of the experiment is more likely due to an isotopic exchange with the oxygen in the water than evidence of a process.

Reply: Whether the drop is solely caused by the O isotopic exchange or, maybe partially, by interactions with the mineral surface, is not really clear. The drop observed in $\delta^{18}\text{O}$ occurs almost simultaneously with the e.g. the decrease in $\delta^{15}\text{N}$ for the mineral + dead biomass experiment. This might be indicative of other processes playing indeed a certain role. However, as we tried to explain in L496ff in the original MS, we assume that the main effect is the oxygen exchange with the water of the medium, which simply takes time and thus results in “fluctuations” (especially for the mineral only experiments) until the entire system is equilibrated.

L531-538: It might be interesting to look at $\delta^{18}\text{O}$ variations of N_2O during the experiment. And see if it correlates with that of nitrite. This would also be an opportunity to confirm or deny whether there is an isotope exchange between the oxygen in the nitrite and the oxygen in the water.

Reply: Indeed, using the $\delta^{18}\text{O}$ variations of N_2O might help to better understand the isotope exchange processes within the system. However, since N_2O is definitely not the only product and possibly further

reduced (resulting in a branching effect caused by the removed O atoms, which is further affecting the O dynamics within the system), this approach would be biased.

L551-552: if N₂O is considered to accumulate, it can be considered to be the accumulated product in the case of a Rayleigh distillation. In this case, and taking into account the isotope fractionation associated with nitrite reduction, it is easy to calculate what the expected ¹⁵N and ¹⁸O of the N₂O produced. It would then be interesting to compare the measured values with the expected values.

Reply: We agree that it is indeed possible to estimate the predicted value of $\delta^{15}\text{N}$ by using the accumulated product equation. An epsilon value calculated from the $\delta^{15}\text{N-NO}_2^-$ data could be used to estimate the predicted $\delta^{15}\text{N-N}_2\text{O}$ values, which would be different since N₂O is clearly not the single product. However, for $\delta^{18}\text{O}$ this approach would not work due to the branching effect occurring during reduction. Hereby, the O atoms get plucked off and lost along the reaction, which is also affecting the dynamics.

At the editor's discretion, and if the manuscript is not already considered too long, we would be happy to add the "predicted" $\delta^{15}\text{N-N}_2\text{O}$ values with a short explanation.

1.2. Response to comments by Anonymous Referee #2

First, we would like to thank the reviewer for his/her valuable inputs and comments on our manuscript. We have to admit that the outliers in the N₂O data are indeed real outliers due to a "concentration/linearity effect" during the measurement in which overly large peak areas in the raw data biased the results. After a thorough check of the raw data, these few data points were removed and the graphs were re-drawn. We contend the data now presented are valid and accurate. We apologize for the mistake.

L98: "hold the potential to disentangle abiotic and biotic NO₂- reduction " - this cannot be concluded from the previous sentences, which say that for both biotic and abiotic processes we deal with significant isotope effect

Reply: We will rephrase that part.

L184: "flushed before for 5 hrs with 5.0 He" - is this right - you need to flush 5hrs? Why so long? Have you tested that this is needed?

Reply: Since we simply applied the flushing routine of the denitrifier method, the headspace vials were indeed flushed for 5 hrs. Later testing showed, that 3 hrs would also suffice. However, several hours of flushing seem to be necessary to reduce the blank value to acceptable levels, in particular when sample size is low.

L315: you mean Fig. 6 here?

Reply: We thank the reviewer for pointing this out and apologize for the mistake! Indeed, in L315 it should indeed read Fig. 6. We will change this in the manuscript!

L315: Such a value seems rather not plausible, please double check your measurements and check how reliable is this value. There is no known process which could result in such negative value. Similarly, in 6C - I'd even doubt the value of -40 permil, unless you have ideas to explain this.

Reply: As already mentioned, we carefully checked the raw data as well as the corrected data files again and we have to admit that these values are indeed outliers caused by very high peak areas (concentration effect). We corrected the graphs accordingly (see graph attached).

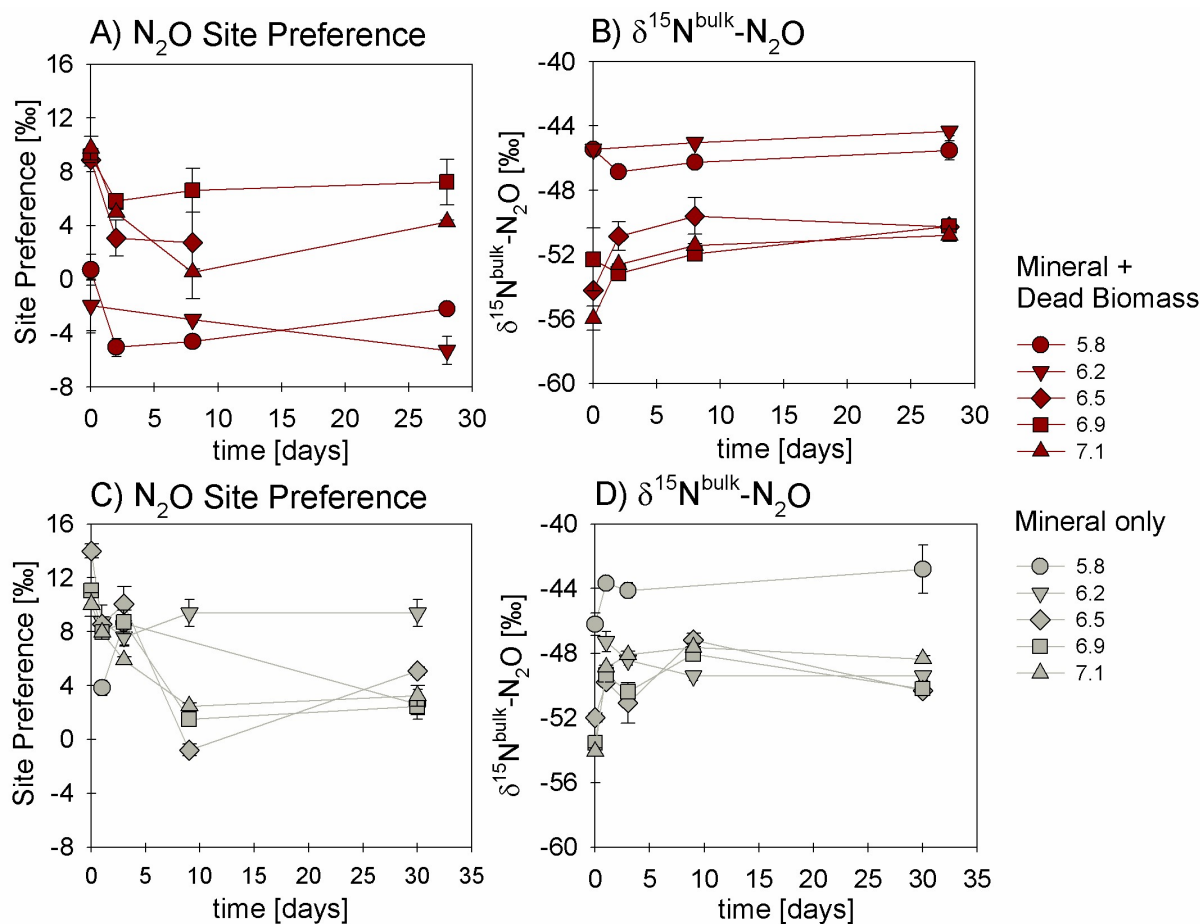


Figure 3: Same as Figure 2 - Site Preference (SP; A, C) and $\delta^{15}\text{N}^{\text{bulk}}\text{-N}_2\text{O}$ (B, D) values of N_2O produced in experiments amended with mineral + dead biomass (red) and mineral-only (grey)

L346: Is further N_2O reduction to N_2 also possible? If not, please explain why.

Reply: Considering previous publications (Rivallan et al., 2009; Doane, 2017; Phillips et al, 2016), an abiotic reduction of N_2O to N_2 is indeed possible, particularly in the presence of a reactive surface.

See L559-570: “Abiotic decomposition of N_2O to N_2 in the presence of Fe-bearing zeolites has been investigated previously (Rivallan et al., 2009). However, it remains unclear if this process could also occur here. Fractional N_2O reduction is also not explicitly indicated by the SP values, which would reflect an increase with N_2O reduction (Ostrom et al., 2007; Winther et al., 2018) [...] However, since N_2O concentrations, even if minor, are increasing towards the end of the experiments, production and possible decomposition as well as ongoing sorption mechanisms might also serve as possible explanation leading to these rather low SP values.”

However, with regards to the rather low N_2O concentrations and given the relatively constant $\delta^{15}\text{N}^{\text{bulk}}\text{-N}_2\text{O}$ values, abiotic N_2 production seems plausible. First, the N_2O produced here accounts only for $\sim 0.7\%$ of the total NO_2^- reduced in the experiments. This large difference might be caused by sorption processes or simply by the fact that N_2O is not the final product (Note: accumulation of the intermediates e.g. NO , is quite unlikely since they are extremely reactive). Furthermore, if N_2O were indeed the final and only product, its $\delta^{15}\text{N}^{\text{bulk}}$ values should approximate the $\delta^{15}\text{N}\text{-NO}_2^-$ values (starting off lighter than $\delta^{15}\text{N}\text{-NO}_2^-$ and increasing over incubation time). However, here the $\delta^{15}\text{N}^{\text{bulk}}\text{-N}_2\text{O}$ values remained relatively steady or did not increase much throughout the experiment, which might indicate that N_2O is not just produced but possibly also further reduced (multistep-reaction). Therefore, the production of N_2 , although abiotic, seems quite likely. We clarify this in the revised MS.

As written in L597-601: “Considering that the N₂O concentrations measured in our experiments were comparatively low and that $\delta^{15}\text{N}^{\text{bulk}}\text{-N}_2\text{O}$ values did not noticeably change throughout the experiments, formation of N₂ via abiotic interactions between NO₂⁻ and NO may also be involved (Doane, 2017; Phillips et al., 2016). Hence, N₂O is possibly involved in the reaction either as an intermediate or as a side product, and can thereby influence the overall N and O isotope dynamics.”.

L484: This is not clear: $\delta^{15}\text{N}$ decrease and initial decrease?

Reply: Here, we meant the decrease in $\delta^{15}\text{N}$ and an observed initial decrease in the concentration of NO₂⁻. We will add “concentration” to avoid further confusion.

L547: "was calculated is based" - sentence to be rewritten

Reply: Again, we thank the reviewer for reading our manuscript so carefully. This will of course be corrected.

L548: What do the arrows mean? (in table 3)

Reply: The arrows were added to indicate an overall increase (↑) or decrease (↓) from the initial delta value. We will correct a mistake (line for $\delta^{15}\text{N}\text{-NO}_2^-$ values - arrow for DB + mineral setup should point up) that we only now detected, and we will add the explanation in the caption of the table.

L614: This last sentence is not stated in the discussion - in discussion you just say it is unsure if abiotic N₂ production is possible. Please explain this more detailed.

It is not said in the discussion what is the isotope effect of abiotic N₂O reduction to N₂ (is this known?) - so I do not understand how N₂O isotopic results can suggest its occurrence.

Reply: Generally, N₂ production is still assumed to be caused mainly by enzymatic reactions. However, there are studies providing evidence for abiotic N₂ production (e.g. Rivallan et al., 2009; Phillips et al., 2016). In our manuscript, we choose to only cautiously refer to the possible abiotic N₂O reduction to N₂, since most N cycling studies still do not account for abiotic N₂ production. Furthermore, our SP values do not explicitly indicate the occurrence of fractional N₂O reduction (N₂O accumulates, SP values remain rather steady). Unfortunately, we did not analyse N₂ samples, hence we do not know the range of N₂ concentrations and/or isotope values, which would help to better address this aspect.

To the best of our knowledge, the isotope effect of abiotic N₂O reduction to N₂ is unknown. As already mentioned above, N₂O accumulates throughout the experiments but overall accounts only for a small fraction of the NO₂⁻ reduced. Furthermore, the $\delta^{15}\text{N}^{\text{bulk}}\text{-N}_2\text{O}$ values remained rather steady throughout the experiments, which indicates that other processes may influence the reaction dynamics and that N₂O may simply be an intermediate. If, again, N₂O were the final and only product, $\delta^{15}\text{N}^{\text{bulk}}$ values would be expected to increase with decreasing NO₂⁻ concentrations (and thus increasing $\delta^{15}\text{N}\text{-NO}_2^-$). However, $\delta^{15}\text{N}^{\text{bulk}}\text{-N}_2\text{O}$ values do not really change much toward the end of the experiments, and remain steady for quite some time. Thus they do not reflect the patterns expected for a final product.

2. List of relevant changes

2.1. Adjustments according to our responses to comments by anonymous Referee #1

- L147 Sampling procedure details added; “within one hour after the sample was taken via a...”
- L150 Ferrozine analysis details added; “SFA- and/or HCl-fixed samples were stored in the dark and at 4°C until”
- L153 Procedure details added; “Triplicate samples”

- L179f Procedure details added; "...upside down at room temperature and in the dark. Two nitrite isotope standards, namely (N-7373 ($\delta^{15}\text{N}$: -79.6‰, $\delta^{18}\text{O}$: +4.5‰) and N-10219 ($\delta^{15}\text{N}$: +2.8‰; $\delta^{18}\text{O}$: +88.5‰); (Casciotti & McIlvin, 2007)..."
- L182 Sentence added: "Based on replicate measurements of laboratory standards and samples, the analytical precision for NO_2^- $\delta^{15}\text{N}$ and $\delta^{18}\text{O}$ analyses was $\pm 0.4\%$ and $\pm 0.6\%$ (1 SD), respectively."
- L213 Added reference to Figure S4 added (S4 – requested Figure, added to the supplementary information)
- L303 Figure 5, x-axis title changed to " $\ln(f)$ "
- L316 Figure 6 replaced with a corrected version; Caption changed to "...For pH 6.5, the final SP value (A) is missing due to analytical problems (overly large sample peak areas). Standard error calculated from biological replicates ($n = 3$ or 2) is represented by the error bars."
- L321-327 References to Figures S5 and S6 changed to S6 and S7, respectively
- L598ff Changed to "Considering that the N_2O concentrations measured in our experiments were comparatively low and that $\delta^{15}\text{N}^{\text{bulk}}\text{-N}_2\text{O}$ values did not noticeably change throughout the experiments, it is **unlikely that N_2O is the final product**, and formation of N_2 via abiotic interactions between NO_2^- and NO is probably also involved (Doane, 2017; Phillips et al., 2016). Indeed, if **accumulated as the final product, the $\delta^{15}\text{N}^{\text{bulk}}\text{-N}_2\text{O}$ value at the end of the incubation should be $\sim 33\%$ (according to closed-system accumulated-product Rayleigh dynamics), significantly higher than what we measured ($\sim -50 \pm 6\%$)**. Hence, whether N_2O is an intermediate or parallel side product, its role in the overall reaction complicates N and O isotope mass balance dynamics in complex ways."

2.2. Adjustments according to our responses to comments by anonymous Referee #2

- L98-100 "This suggests that coupled N and O isotope measurements hold the potential to disentangle abiotic and biotic NO_2^- reduction in the presence of Fe(II) ." changed to "However, reaction kinetics can significantly affect isotope reaction dynamics, and chemodenitrification is possibly impacted by e.g. concentration effects and/or the presence of different catalysts (i.e. surfaces, organics). Hence, performing coupled N and O isotope measurements might help to gain deeper insights into the mechanistic details and fractionation systematics of NO_2^- reduction in the presence of Fe(II) ."
- L315 "(Figure 5 A,C)" replaced by "(Figure 6 A, C)"
- L316 Figure 6 replaced with a corrected version; Caption changed to "...For pH 6.5, the final SP value (A) is missing due to analytical problems (overly large sample peak areas). Standard error calculated from biological replicates ($n = 3$ or 2) is represented by the error bars."
- L484f "...was observed with the initial decrease..." changed to "...occurred in parallel contemporaneously with initially decreasing in NO_2^- concentrations."
- L545ff Table 3 – Caption corrected (plus values): " $\delta^{15}\text{N}$ and $\delta^{18}\text{O}$ values were calculated using $\bar{x}_{t0} - \bar{x}_{tend}$. Isotope fractionation was calculated is based on the slope between the lowest initial value (here at t_1) and tend for all pH." changed to " $\delta^{15}\text{N}$ and $\delta^{18}\text{O}$ values were calculated using $\bar{x}_{t0} - \bar{x}_{tend}$, whereas an overall increase from the initial value is marked with \uparrow , and a decrease with \downarrow . The calculated isotope fractionation factor (ϵ) is based on the slope between the lowest initial value (here at t_1) and t_{end} for all pH."
- L598ff Changed to "Considering that the N_2O concentrations measured in our experiments were comparatively low and that $\delta^{15}\text{N}^{\text{bulk}}\text{-N}_2\text{O}$ values did not noticeably change throughout the experiments, **it is unlikely that N_2O is the final product, and formation of N_2 via abiotic interactions between NO_2^- and NO is probably also involved** (Doane, 2017; Phillips et al., 2016). Indeed, if accumulated as the final

product, the $\delta^{15}\text{N}^{\text{bulk}}\text{-N}_2\text{O}$ value at the end of the incubation should be $\sim 33\%$ (according to closed-system accumulated-product Rayleigh dynamics), significantly higher than what we measured ($\sim -50 \pm 6 \%$). Hence, whether N_2O is an intermediate or parallel side product, its role in the overall reaction complicates N and O isotope mass balance dynamics in complex ways.“

2.3. General Adjustments

L48	L55 to 65 moved upwards, removed L48 to L50
L50f	Sentence merged with first part of the next sentence
L53	Added “EPS has been demonstrated to...”
L55	“biologically” changed to “enzymatically”
L70	Reference added (Zhu-Barker et al., 2012)
L203	Figure 1: Caption corrected – pH 5.8
L235	“lost” changed to “processing failed”
L251	Added “sample processing failed for the”, removed “was lost”
L291	Added reference to Figure 4 C
L295	(Figure S4) Rayleigh plot for mineral only experiments now added to Supplementary information file
L309	“amended” replaced with “mineral plus DB”; “(SP)” added after “Site preference”
L314f	SP values in text replaced with corrected values
L356-358	Sentence deleted
L451-454	Sentence deleted
L532	“...(abiotic $-46.5 \pm 0.2\%$; dead biomass $-49.4 \pm 1.0\%$)...” changed to “...(abiotic $-49.5 \pm 0.6\%$; dead biomass $-50.5 \pm 0.8\%$)...”
L555	“mineral-only treatment (27.9%) is only slightly higher than that of the DB experiment (23.2%),“ changed to “mineral-only treatment (30.9%) is slightly higher than that of the DB experiment (24.4%)”
L562f	“relatively low ($6.0 \pm 0.8\%$; $1.7 \pm 1.2\%$; Fig. 6) “ changed to “relatively low ($6.5 \pm 0.8\%$; $2.3 \pm 1.2\%$; Fig. 6, Table 3).”
L602	Figure 8 slightly corrected (colours of bonds between species)
L661-664	Acknowledgements corrected (added: Toby Samuels and Louis Rees)
L675ff	Changed formatting of the reference list
Supplements	S4 to S7 were corrected (L20: now S4 – graph depicting N_2O versus NO_2^- concentrations, requested by referee#1; L24 now S5 – Rayleigh plots for the mineral-only setups; L29: now S6 – Rayleigh plots for N_2O $\delta^{15}\text{N}^{\alpha}$, $\delta^{15}\text{N}^{\text{bulk}}$ and site preference, SP; L34: now S7 – Plot showing $\delta^{18}\text{O}$ vs $\delta^{15}\text{N}^{\text{bulk}}$ in N_2O for mineral-only and mineral plus dead biomass setups)

1 Impact of reactive surfaces on the abiotic reaction between nitrite and 2 ferrous iron and associated nitrogen and oxygen isotope dynamics

3 Anna-Neva Visser^{1,4}, Scott D. Wankel², Pascal A. Niklaus³, James M. Byrne⁴, Andreas A. Kappler⁴,
4 Moritz F. Lehmann¹

5 ¹Department of Environmental Sciences, Basel University, Bernoullistrasse 30, 4056 Basel, Switzerland

6 ²Woods Hole Oceanographic Institution, Woods Hole, 360 Woods Hole Rd, MA 02543, USA

7 ³Department of Evolutionary Biology and Environmental Studies, University of Zürich, Winterthurerstrasse 190, 8057 Zürich,
8 Switzerland

9 ⁴Department of Geosciences, Tübingen University, Hölderlinstrasse 12, 72074 Tübingen, Germany

10 Correspondence to: Anna-Neva Visser (a.visser@unibas.ch)

11 **Abstract.** Anaerobic nitrate-dependent Fe(II) oxidation (NDFeO) is widespread in various aquatic environments, and plays a
12 major role in iron and nitrogen redox dynamics. However, evidence for truly enzymatic, autotrophic NDFeO remains limited,
13 with alternative explanations involving coupling of heterotrophic denitrification with abiotic oxidation of structurally-bound
14 or aqueous Fe(II) by reactive intermediate N species (chemodenitrification). The extent to which chemodenitrification is
15 caused, or enhanced, by *ex vivo* surface catalytic effects has, so far, not been directly tested. To determine whether the presence
16 of either a Fe(II)-bearing mineral or dead biomass (DB) catalyses chemodenitrification, two different sets of anoxic batch
17 experiments were conducted: 2 mM Fe(II) was added to a low-phosphate medium, resulting in the precipitation of vivianite
18 ($\text{Fe}_3(\text{PO}_4)_2$), to which later 2 mM nitrite (NO_2^-) was added, with or without an autoclaved cell suspension ($\sim 1.96 \times 10^8$ cells ml^{-1})
19 of *Shewanella oneidensis* MR-1. Concentrations of nitrite, nitrous oxide (N_2O) and iron (Fe^{2+} , Fe_{tot}) were monitored over
20 time in both setups to assess the impact of Fe(II) minerals and/or DB as catalysts of chemodenitrification. In addition, the
21 natural-abundance isotope ratios of NO_2^- and N_2O ($\delta^{15}\text{N}$ and $\delta^{18}\text{O}$) were analysed to constrain associated isotope effects. Up
22 to 90% of the Fe(II) was oxidized in the presence of DB, while only ~65% were oxidized under mineral-only conditions,
23 suggesting an overall lower reactivity of the mineral-only setup. Similarly, the average NO_2^- reduction rate in the mineral-only
24 experiments (0.004 ± 0.003 $\text{mmol L}^{-1} \text{day}^{-1}$) was much lower compared to experiments with mineral plus DB (0.053 ± 0.013
25 $\text{mmol L}^{-1} \text{day}^{-1}$), as was N_2O production (204.02 ± 60.29 nmol/L*day). The N_2O yield per mole NO_2^- reduced was higher in
26 the mineral-only setups (4%) compared to the experiments with DB (1%), suggesting the catalysis-dependent differential
27 formation of NO. N- NO_2^- isotope ratio measurements indicated a clear difference between both experimental conditions: In
28 contrast to the marked ^{15}N isotope enrichment during active NO_2^- reduction ($^{15}\epsilon_{\text{NO}_2} = +10.3\%$) observed in the presence of
29 DB, NO_2^- loss in the mineral-only experiments exhibited only a small N isotope effect ($< +1\%$). The NO_2^- -O isotope effect
30 was very low in both setups ($^{18}\epsilon_{\text{NO}_2} < 1\%$), most likely due to substantial O isotope exchange with ambient water. Moreover,
31 during the low-turnover conditions (i.e.; in the mineral-only experiments, as well as initially in experiments with DB), the
32 observed NO_2^- isotope systematics suggest, transiently, a small inverse isotope effect (i.e.; decreasing nitrite $\delta^{15}\text{N}$ and $\delta^{18}\text{O}$)

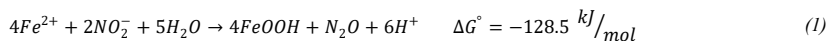
33 with decreasing concentrations), possibly related to transitory surface complexation mechanisms. Site preference (SP) of the
34 ¹⁵N isotopes in the linear N₂O molecule for both setups ranged between 0 to 14‰, notably lower than previously reported for
35 chemodenitrification. Our results imply that chemodenitrification is dependent on the available reactive surfaces, and that the
36 NO₂⁻ (rather than the N₂O) isotope signatures may be useful for distinguishing between chemodenitrification catalysed by
37 minerals, chemodenitrification catalysed by dead microbial biomass, and possibly true enzymatic NDFeO.

38 1. Introduction

39 Iron (Fe) is essential for all living beings and its biogeochemical cycling has been studied extensively (Expert, 2012; Lovley,
40 1997). Although Fe is ubiquitous in most environments, it is not always bioavailable (Andrews et al., 2003; Ilbert and
41 Bonnefoy, 2013), and microorganisms must often cope with Fe limitation in their respective environments (Braun and Hantke,
42 2013; Ilbert and Bonnefoy, 2013). This is especially true at circumneutral pH and oxic conditions, where Fe(II) is quickly
43 oxidized by O₂ and thus only present as poorly soluble Fe(III)(oxyhydr)oxides (Cornell and Schwertmann, 2003; Stumm and
44 Sulzberger, 1992). In contrast, under anoxic conditions, Fe is mainly present as either dissolved Fe²⁺ or as mineral-bound Fe(II)
45 in ~~iron-Fe~~ phosphates or carbonates (Charlet et al., 1990; Luna-Zaragoza et al., 2009). Here, microbes use electron acceptors
46 other than O₂ for respiration (He et al., 2016; Lovley, 2012; Straub et al., 1996). One redox pair that has been proposed to be
47 exploited by microbes under anoxic conditions is NO₃⁻/Fe²⁺, through a mechanism known as nitrate-dependent Fe(II) oxidation
48 (NDFeO) (Ilbert and Bonnefoy, 2013; Straub et al., 1996). ~~To date, indeed, to date, genetic evidence that clearly supports this~~
49 ~~metabolic capacity of the studied microorganisms remains lacking (Price et al., 2018), and biogeochemical evidence is rare~~
50 ~~and putative. The latter is mostly based on experiments with the chemolithoautotrophic culture KS, a consortium of four~~
51 ~~different strains, including a relative of the microaerophilic *Sideroxydans/Gallionella*. This enrichment culture has been shown~~
52 ~~to be able to oxidize Fe(II) without the addition of any organic co-substrates (Tominski et al., 2018). Tian et al. (2020)~~
53 ~~confirmed that *Gallionellaceae* are able to perform autotrophic Fe(II)-dependent denitrification. Another more indirect line of~~
54 ~~evidence includes results from slurry microcosm experiments with marine coastal sediments. In these experiments, Fe(II)~~
55 ~~oxidation was still detected even after all bioavailable organics of the sediments were consumed and only NO₃⁻ was left (Laufer~~
56 ~~et al., 2016). With regards to other studies where NDFeO was initially thought to be performed by autotrophs (Chakraborty et~~
57 ~~al., 2011; Weber et al., 2009), it was subsequently shown that the microbes rely on an organic co-substrate and must in fact be~~
58 ~~considered mixotrophic (Klueglein et al., 2014; Muehe et al., 2009). Yet, the exact mechanism promoting NDFeO in the~~
59 ~~microorganisms that have been investigated so far (e.g. *Acidovorax delafieldii* strain 2AN, *Pseudogulbenkiania ferrooxidans*~~
60 ~~strain 2002) (Chakraborty et al., 2011; Weber et al., 2009), is still not fully understood. Over the past two decades, several~~
61 ~~microorganisms have been investigated and reported to be either chemolithoautotrophic or -mixotrophic nitrate-dependent~~
62 ~~Fe(II)-oxidising bacteria (e.g. *Acidovorax delafieldii* strain 2AN, *Pseudogulbenkiania ferrooxidans* strain 2002) (Chakraborty~~
63 ~~et al., 2011; Weber et al., 2009). It has been suggested that extracellular electron transfer (EET) might play a major role in~~
64 ~~NDFeO, particularly in the presence of high levels of extracellular polymeric substances (EPS) (Klueglein et al., 2014; Liu~~

Kommentiert [AV1]: Moved this part up – might improve “flow”

65 et al., 2018; Zeitvogel et al., 2017). ~~which EPS has been demonstrated to can~~ act as electron shuttles, ~~hence~~ EET may indeed
66 provide a plausible explanation for the observed Fe(II) oxidation in these cultures (Liu et al., 2018). The existence of such an
67 electron transfer would imply that NDFeO is not necessarily a completely ~~biologically-enzymatically~~-catalysed reaction.
68 ~~Indeed, to date, genetic evidence that supports this metabolic capacity of the studied microorganisms remains lacking (Price~~
69 ~~et al., 2018), and biogeochemical evidence is rare and putative. The latter is mostly based on experiments with the~~
70 ~~chemolithoautotrophic culture KS, a consortium of four different strains, including a relative of the microaerophilic~~
71 ~~*Sideroxydans/Gallionella*. This enrichment culture has been shown to be able to oxidize Fe(II) without the addition of any~~
72 ~~organic co-substrates (Tominski et al., 2018). Tian et al. (2020) confirmed that *Gallionellaceae* are able to perform autotrophic~~
73 ~~Fe(II)-dependent denitrification. Another more indirect line of evidence includes results from slurry microcosm experiments~~
74 ~~with marine coastal sediments. In these experiments, Fe(II) oxidation was still detected even after all organics of the sediments~~
75 ~~were consumed and only nitrate was left (Laufer et al., 2016). With regards to other studies where NDFeO was initially thought~~
76 ~~to be performed by autotrophs (Chakraborty et al., 2011; Weber et al., 2009), it was subsequently shown that the microbes rely~~
77 ~~on an organic co-substrate and must in fact be considered mixotrophic (Klueglein et al., 2014; Muehe et al., 2009). Yet, the~~
78 ~~exact mechanism promoting NDFeO is still not fully understood. Considering that all putative NDFeO strains were grown~~
79 under high (up to 10 mM) nitrate (NO₃⁻) and Fe(II) concentrations, and accumulated up to several mM nitrite (NO₂⁻) from
80 enzymatic NO₃⁻ reduction, ~~it was other studies~~ suggested that the observed Fe(II) oxidation in these pure cultures may be due
81 to the abiotic side reaction between the generated NO₂⁻ and Fe(II) (Buchwald et al., 2016; Prakash Dhakal, 2013; Klueglein et
82 al., 2014). This abiotic reaction between NO₂⁻ and Fe(II) is known as chemodenitrification (Equation 1) and is proposed to
83 lead to an enhanced production of N₂O (Anderson and Levine, 1986; Buchwald et al., 2016; Zhu-Barker et al., 2015).



84 Several studies have noted that the presence of reactive surfaces may enhance the abiotic reaction (Heil et al., 2016; Sorensen
85 and Thorling, 1991). For example, Klueglein and Kappler (2013) tested the impact of goethite on Fe-coupled
86 chemodenitrification in the presence of high Fe(II) and NO₂⁻ concentrations, and confirmed the concentration dependency of
87 this reaction with regard to both species (Van Cleemput and Samater, 1995). Possible catalytic effects (e.g. by reactive surfaces
88 and/or organic matter) were not tested specifically in these studies. Yet, multiple factors have been shown to affect the abiotic
89 reaction between NO₂⁻ and Fe(II) and may need to be considered (i.e.: pH, temperature, Fe²⁺ concentrations, solubility of
90 Fe(III)(oxyhydr)oxides, crystallinity of Fe(II) minerals, other metal ion concentrations and catalytic effects) (Van Cleemput
91 & Samater, 1995; Klueglein & Kappler, 2013; Ottley et al., 1997). In addition, the presence of organic compounds can lead to
92 the abiotic reduction of NO₂⁻ to NO (Van Cleemput and Samater, 1995; McKnight et al., 1997; Pereira et al., 2013).
93 Given the complex controls and potential interaction between Fe(II) and various nitrogenous compounds, including
94 intermediates, it may be an oversimplification to state that Fe(II) oxidation observed in previous laboratory setups is solely
95 caused by the abiotic reaction with NO₂⁻, and not, for example, stimulated by reactive surfaces (minerals, organic-detritus) or
96 by nitric oxide (NO), a highly reactive intermediate not easily quantified in anoxic experiments. In order to better understand

97 the factors that may control chemodenitrification of NO_2^- , this study focuses on the possible catalytic surface effects induced
98 by a Fe(II) mineral phase or dead biomass (DB). Furthermore, microbial cells, dead biomass DB, or detrital waste products
99 might not only provide additional reactive surface area, but may directly react with NO_2^- to form NO.

100 Stable isotopes of both N and O ($\delta^{15}\text{N}$ and $\delta^{18}\text{O}$) offer a promising approach to further elucidate the mechanism of NDFeO,
101 and also to more generally expand our understanding of chemodenitrification. The N and O isotopic composition of
102 nitrogenous compounds (e.g., NO_3^- , NO_2^- , and N_2O) has been used to gain deeper insights into various N turnover processes
103 (Granger et al., 2008; Jones et al., 2015). The dual NO_2^- (or NO_3^-) isotope approach is based on the fact that specific N-
104 transformation processes – biotic or abiotic – are associated with specific N and O isotope fractionation (i.e., isotope effect).
105 In general, enzymatic processes promote the more rapid reaction of lighter N and O isotopologues, leaving the remaining
106 substrate pool enriched in the heavier isotopes (i.e., ^{15}N , ^{18}O) (Granger et al., 2008; Kendall & Aravena, 2000; Martin &
107 Casciotti, 2017). Only a few studies exist that have looked into the isotope effects of chemodenitrification and reports on the
108 associated isotope effects are variable. Consistent with what we know from biological denitrification, chemodenitrification
109 experiments with 10 mM Fe(II) and NO_2^- , with very high reaction rates, revealed a significant increase in the $\delta^{15}\text{N}$ (up to 40%)
110 and $\delta^{18}\text{O}$ (up to 30%) NO_2^- values, corresponding to an overall N and O isotope effect of $^{15}\epsilon$ $18.1 \pm 1.7\%$ and $^{18}\epsilon$ $9.8 \pm 1.8\%$,
111 as well as a $\Delta^{15}\text{N}$ (i.e., the difference between $\delta^{15}\text{NO}_2^-$ and $\delta^{15}\text{N}_2\text{O}$) of $27 \pm 4.5\%$ (Jones et al., 2015). However, since reaction
112 kinetics are able to meddle with the can significantly affect isotope reaction dynamics, and chemodenitrification is possibly
113 impacted by e.g. the concentration effect-concentration effects and/or the presence of different catalysts (i.e. surfaces,
114 organics). Hence, performing This suggests that coupled N and O isotope measurements might help to gain deeper insights
115 into the mechanistic details and fractionation dynamics-systematics of hold the potential to disentangle abiotic and biotic- NO_2^-
116 reduction in the presence of Fe(II). Here, in order to expand the limited dataset on the isotope effects of abiotic Fe(II)-coupled
117 denitrification, and in turn to lay the groundwork for using $\text{NO}_3^-/\text{NO}_2^-$ N and O isotope measurements to unravel the mechanism
118 behind NDFeO, we studied the N and O isotope dynamics of NO_2^- reduction and N_2O production during abiotic reaction of
119 NO_2^- with Fe(II). As the extent of the formation of various Fe(III)(oxyhydr)oxides has been previously reported to enhance
120 chemodenitrification dynamics (Chen et al., 2018; Sorensen and Thorling, 1991), we also followed mineral alteration during
121 chemodenitrification in order to identify possible reaction patterns. A specific goal in this context was to assess the impact of
122 Fe(II) precipitates and/or dead biomass as catalytic agents during Fe(II)-associated chemodenitrification, as well as potential
123 mineral transformation processes associated with the abiotic oxidation of Fe(II) via reactive NO_x species.

124 2. Material and Methods

125 2.1. General experimental setup

126 For all experiments, anoxic low phosphate medium (1.03 mM KH_2PO_4 , 3.42 mM NaCl, 5.61 mM NH_4Cl , 2.03 mM $\text{MgSO}_4 \cdot 7$
127 H_2O and 0.68 mM $\text{CaCl}_2 \cdot 2 \text{H}_2\text{O}$, with a 7-vitamin (Widdel & Pfennig, 1981) and a SL-10 trace element solution (Widdel et
128 al., 1983); 22 mM bicarbonate buffered) was prepared. The medium was dispensed with a Widdel flask in 1-l Schott bottles

129 and the pH for each bottle was adjusted separately by the addition of anoxic, sterile 1 M HCl. For ~~the~~ both setups, five different
130 pH values were targeted: 5.8, 6.2, 6.5, 6.9 and 7.1. After pH adjustment, Fe(II)Cl₂ was added to reach a concentration of ~2
131 mM Fe(II), and, if necessary, the pH was re-adjusted. The medium was kept for 48 h at 4°C, resulting in amorphous, green-
132 greyish Fe(II) precipitates. In addition, ~2 mM NaNO₂ and ~1 mM Na-acetate were added to the main medium stocks shortly
133 before 10 ml aliquots of the medium were distributed into 20 ml headspace vials (heat-sterilized) in an anoxic glove box
134 (MBraun, N₂, 100%). Acetate was added to mimic experiments, in which bacteria are cultivated (yet, acetate concentrations
135 did not change during incubations, underscoring that the organic acid was not involved in the observed reactions; data not
136 shown). All headspace vials were closed with black butyl stoppers and crimp-sealed [headspace N₂/CO₂ (90/10, v/v)]. All vials
137 were then incubated at 28°C in the dark.

138 *Incubations with dead-biomass* – *Shewanella oneidensis* MR-1, a facultatively aerobic Gram-negative bacterium, is seen as
139 model organism for bioremediation studies due to its various respiratory abilities (Heidelberg et al., 2002; Lies et al., 2005). It
140 is known to perform dissimilatory metal reduction by utilizing alternative terminal electron acceptors such as elemental sulfur,
141 Mn(IV), Fe(III) or NO₃⁻. Since *S. oneidensis* produces large amounts of EPS (Dai et al., 2016; Heidelberg et al., 2002), but is
142 not capable of oxidizing Fe(II) (Lies et al., 2005; Piepenbrock et al., 2011) (i.e. no interference with abiotic reactions involving
143 Fe/chemodenitrification), we chose concentrated and sterilized *S. oneidensis* for our dead-biomass experiments. In preparation
144 of these experiments, *S. oneidensis* MR-1 was grown oxically on a LB (lysogeny broth) medium (10 g tryptone, 5 g yeast
145 extract, 10 g NaCl in 1 l DI water) in six 250 ml Erlenmeyer flasks. After 12 hrs, cultures were transferred into 50 ml Falcon
146 tubes and centrifuged for 25 min at 4000 rpm (Eppendorf, 5430 R). Cell-containing pellets were washed twice with oxalic acid
147 and centrifuged again, followed by three more washing steps with TRIS buffer prior to final resuspension in 5 ml TRIS buffer.
148 Pellet suspensions were pooled in a 100 ml serum bottle and autoclaved twice to ensure that all cells were killed. Before
149 distribution of the medium into 20 ml vials (see above), cell suspension was added to yield a cell density of ~1.96×10⁸ cell ml⁻¹.
150 Care was taken to ensure the homogenous distribution of mineral precipitates and the dead biomass.

151 2.2. Sampling and sample preparation

152 Incubations were run for approximately 30 days, and sampling was performed in an anoxic glove box (MBraun, N₂, 100%) at
153 five time points. For each time point, and for each pH treatment, 9 replicates were prepared. Therefore, variations between the
154 replicates and the different sampling time points are possible. For sampling, the headspace was quantitatively transferred into
155 12 ml He-purged Exetainer vials (LABCO) for N₂O concentration measurements. Then, 2 ml of the liquid sample were
156 transferred into 2 ml Eppendorf tubes, centrifuged for 5 min (13400 rpm; Eppendorf, MiniSpin), followed by a 1:10 dilution
157 of the supernatant in 1 ml anoxic MilliQ water for NO₂⁻ quantification. A second 100 µl aliquot was diluted 1:10 in 40 mM
158 sulfamic acid (SFA) for iron determination by ferrozine analysis (Granger and Sigman, 2009; Klueglein and Kappler, 2013).
159 The remaining supernatant was used for HPLC and NO₂⁻ isotope analysis. Finally, the spun-down pellet was resuspended in 1
160 M HCl for ferrozine analysis (Stokey, 1970). All liquid samples were stored at 4°C in the dark until further processing. The
161 remaining liquid samples were used for ⁵⁷Fe Mössbauer spectroscopy.

162 2.3. Analytical techniques

163 NO_2^- concentrations – NO_2^- concentrations were quantified within one hour after the sample was taken via using a standard
164 segmented continuous-flow analytical (CFA, SEAL Analytics) photometric techniques (Snyder and Adler, 1976). NO_2^-
165 reduction rates were calculated based on the observed net concentration decrease ($[\overline{C}]_{t_0} - [\overline{C}]_{t_{end}} \pm \text{standard error}$) with time.

166 Fe concentrations – SFA- and/or HCl-fixed samples were stored in the dark and at 4°C until Fe(II) concentrations was/were
167 analysed using the ferrozine assay (Stookey, 1970), which was adapted for NO_2^- -containing samples by Klueglein et al. (2013).
168 Total Fe(II) concentrations were calculated as the sum of the $\text{Fe}_{aq}^{2+} + \text{Fe(II)}_{\text{pellet}}$ concentrations.

169 N_2O concentrations – Prior to the quantification of the N_2O , the sample gas was diluted (1:5) with 5.0 He. The samples
170 (triplicate samples) were then analysed using a gas chromatograph with an electron capture detector (GC-ECD; Agilent
171 7890 with micro-ECD and FID; Porapak Q 80/100 column). GC-ECD measurements were calibrated using four standard gases
172 containing different concentrations of N_2O (Niklaus et al., 2016). N_2O production rates were calculated based on the observed
173 net N_2O concentration increase ($[\overline{C}]_{t_{end}} - [\overline{C}]_{t_0} \pm \text{standard error}$) with time.

174 ^{57}Fe Mössbauer spectroscopy - For Mössbauer spectroscopic analyses, the remaining liquid samples (ca. 8 ml) were processed
175 inside an anoxic glove box. The entire liquid including the precipitates was passed through a 0.45 μm filter. The wet filter was
176 then sealed between two layers of Kapton tape and kept inside sealed Schott bottles in a freezer (-20°C) under anoxic conditions
177 until analysis. From the treatments with DB, samples were collected at day 0 at pH 6.8 and at the end of the experiment (~30
178 days) for pH 6.8 and 5.8. For the mineral-only experiment, only one sample (time point zero, pH 6.8) was analysed, as a basis
179 for comparison with the DB experiments (i.e., to verify whether DB has an immediate effect on the mineral phase). Taking
180 care to minimize exposure to air, samples were transferred from the air-tight Schott bottles and loaded inside a closed-cycle
181 exchange gas cryostat (Janis cryogenics). Measurements were performed at 77 K with a constant acceleration drive system
182 (WissEL) in transmission mode with a $^{57}\text{Co}/\text{Rh}$ source and calibrated against a 7 μm thick $\alpha\text{-}^{57}\text{Fe}$ foil measured at room
183 temperature. All spectra were analysed using Recoil (University of Ottawa) by applying a Voight Based Fitting (VBF) routine
184 (Lagarec and Rancourt, 1997; Rancourt and Ping, 1991). The half-width at half maximum (HWHM) was fixed to a value of
185 0.130 mm/s during fitting.

186 Nitrite N and O isotope measurements – The nitrogen (N) and oxygen (O) isotope composition of NO_2^- was determined using
187 the azide method (McIlvin and Altabet, 2005). This method is based on the chemical conversion of NO_2^- to gaseous N_2O at a
188 low pH (4 to 4.5) (McIlvin and Altabet, 2005), and the subsequent analysis of the concentrated and purified N_2O by gas
189 chromatography— isotope ratio mass spectrometry (GC-IRMS). Addition of 0.6 M NaCl to the acetic acid-azide solution was
190 conducted in order to minimize oxygen isotope exchange (McIlvin and Altabet, 2005). The acetic acid-azide solution was
191 prepared freshly every day (McIlvin and Altabet, 2005) and kept in a crimp sealed (grey butyl stopper) 50 ml serum bottle.
192 Sample volume equivalent to 40 nmol NO_2^- was added to pre-combusted headspace vials, filled up to 3 ml with anoxic MilliQ
193 water, and crimp-sealed. Then, 100 μl of the acetic acid/azide solution was added. After ~7 hrs, 100 μl of 6 M NaOH was
194 added to stop the reaction. Until isotope analysis by a modified purge and trap gas bench coupled to CF-IRMS (McIlvin and

195 Casciotti, 2010), the samples were stored upside down at room temperature and in the dark. Two nitrite isotope standards,
196 namely (N-7373 ($\delta^{15}\text{N}$: -79.6‰, $\delta^{18}\text{O}$: +4.5‰) and N-10219 ($\delta^{15}\text{N}$: +2.8‰; $\delta^{18}\text{O}$: +88.5‰)(Casciotti & McIlvin, 2007), were
197 prepared on the day of isotope analysis and processed the same way as samples. N and O isotope data are expressed in the
198 common δ notation and reported as per mil deviation (‰) relative to AIR N₂ and VSMOW, respectively ($\delta^{15}\text{N} = ([^{15}\text{N}]/$
199 $^{14}\text{N}]_{\text{sample}} / [^{15}\text{N}]/[^{14}\text{N}]_{\text{air, N}_2} - 1) \times 1000\text{‰}$ and $\delta^{18}\text{O} = ([^{18}\text{O}]/[^{16}\text{O}]_{\text{sample}} / [^{18}\text{O}]/[^{16}\text{O}]_{\text{VSMOW}} - 1) \times 1000\text{‰}$). Based on replicate
200 measurements of laboratory standards and samples, the analytical precision for NO₂⁻ $\delta^{15}\text{N}$ and $\delta^{18}\text{O}$ analyses was $\pm 0.4\text{‰}$ and
201 $\pm 0.6\text{‰}$ (1 SD), respectively.

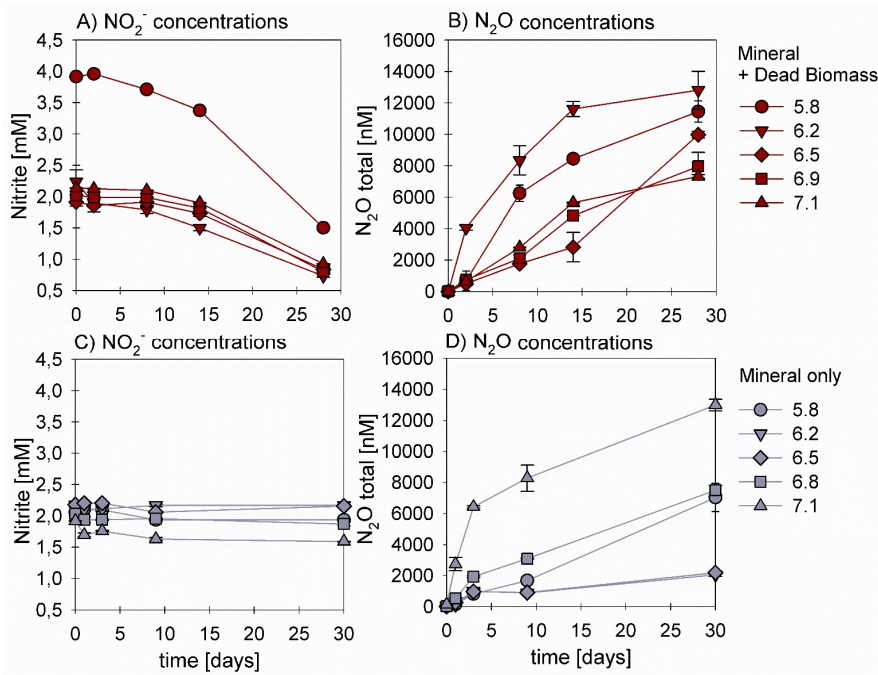
202 *N₂O N and O isotope measurements* – Triplicate 12 nmol samples of N₂O were injected into 20 ml headspace vials that were
203 flushed before for 5 hrs with 5.0 He (injection volumes according to the N₂O concentrations determined before). The N₂O was
204 then analysed directly using CF-IRMS (see above). Two standard gases with known $\delta^{15}\text{N}$ and $\delta^{18}\text{O}$ values were analysed along
205 with the samples, namely FLCA06261 ($\delta^{15}\text{N}$: -35.74‰, $\delta^{15}\text{N}^{\alpha}$: -22.21‰, $\delta^{15}\text{N}^{\beta}$: -49.28‰, $\delta^{18}\text{O}$: 26.94‰) and FI.53504 ($\delta^{15}\text{N}$:
206 48.09‰, $\delta^{15}\text{N}^{\alpha}$: 1.71‰, $\delta^{15}\text{N}^{\beta}$: 94.44‰, $\delta^{18}\text{O}$: 36.01‰) (provided by J. Mohn, EMPA; e.g. Mohn et al., 2014). The gases
207 were calibrated on the Tokyo Institute of Technology scale for bulk and site-specific isotopic composition (Ostrom et al., 2018;
208 Sakae Toyoda et al., 1999). Ratios of m/z 45/44, 46/44 and the 31/30 signals were used to calculate values of $\delta^{15}\text{N}^{\text{bulk}}$
209 (referenced against AIR-N₂), $\delta^{18}\text{O}$ (referenced against V-SMOW), and site-specific $\delta^{15}\text{N}^{\alpha}$, $\delta^{15}\text{N}^{\beta}$ based on Frame and Casciotti
210 (2010). Site preference (SP) was calculated as $\delta^{15}\text{N}^{\alpha} - \delta^{15}\text{N}^{\beta}$ (Sutka et al., 2006; Toyoda and Yoshida, 1999).

211 2.4. Pourbaix diagram

212 In order to predict the stability and behaviour of the N- and Fe(II)-bearing chemical species in the same system, a Pourbaix
213 (Eh-pH) diagram was constructed (Delahay et al., 1950) as a valuable tool to predict possible reactions and speciation of end
214 products under different experimental conditions. To calculate the enthalpies for the stepwise reduction of nitrite during
215 denitrification, as well as Fe(II) oxidation reactions, standard enthalpy values were taken from different references (Table S1).
216 The Pourbaix diagram presented in the discussion was devised using concentrations measured during the experiments
217 performed for this study.

218 3. Results

219 3.1. Chemodenitrification kinetics

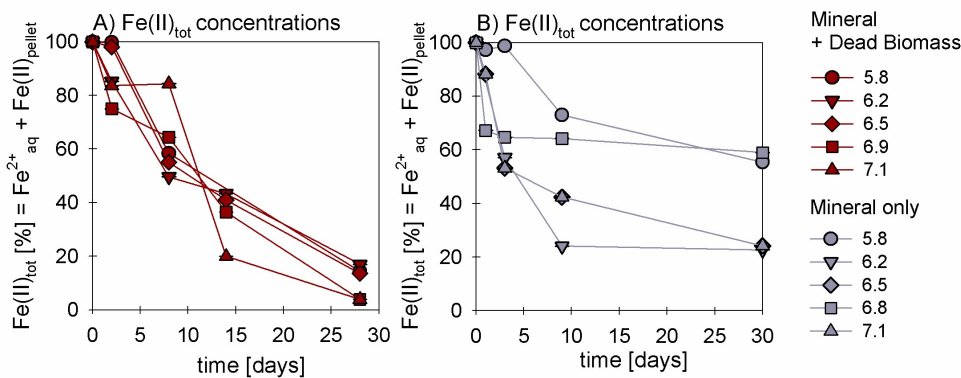


220 Figure 1: Nitrite reduction (A, C) and N₂O production (B, D) over time in the mineral + dead biomass (red) and mineral-only (grey)
 221 setups over time and at different pH. Please note that at pH 5.8 twice the amount of nitrite was accidentally introduced. Standard
 222 error calculated from biological replicates (n = 9) is represented by the error bars.
 223

224 In the presence of DB, NO₂⁻ reduction rates were much higher compared to the mineral-only setup (Figure 1 A, C), with up to
 225 ~60% of the initially amended NO₂⁻ being transformed during the incubation period, independent of the pH. The addition of
 226 DB led to a decrease in NO₂⁻ concentrations from 2 mM to ~0.7 mM (Figure 1 A). The pH 5.8 treatment (unintentionally
 227 amended with 2x NO₂⁻) also showed a similar fractional reduction. In the mineral-only setups the decrease in NO₂⁻
 228 concentration was rather moderate and ranged between 0.3 (pH 7) and 0.1 mM (at lower pH) (Figure 1 C). In all treatments,
 229 N₂O was produced but accounted for a maximum of only 0.7% of the NO₂⁻ consumed. The final N₂O yield per mole NO₂⁻
 230 reduced tended to be lower in the mineral plus DB versus the mineral-only amended setups for most of the pH (Figure 1 B vs.
 231 D). Highest N₂O production was observed at circumneutral pH (7.1) in the mineral-only setup, while maximum final N₂O

232 concentrations were observed at lower pH (6.2) in the incubations with DB (Figure 1 B; S4). A systematic pH effect, however,
 233 could not be discerned. Fe(II)_{total} concentrations rapidly decreased in both setups. In the presence of DB, Fe(II)_{total} oxidation
 234 was almost complete (Figure 2A), independent of the pH, whereas in the mineral-only experiment, Fe(II)_{total} decreased during
 235 the first 5-10 days but then seemed to reach a steady state (Figure 2 B). At pH 6.8 and 5.8, only 40% of the Fe(II)_{total} was
 236 oxidized, whereas at the other pH up to 80% of the Fe(II)_{total} initially amended was oxidized. Total Fe decreased over time
 237 (Figure S2).

Kommentiert [AV2]: That's the additional graph requested by Ref#1



238
 239 **Figure 2: Oxidation of total Fe(II) over time given (reported as % of initial concentration) in the mineral + dead biomass amended**
 240 **(red) and the mineral-only setup (grey), tested at different pH. Standard error calculated from biological replicates (n = 9) is**
 241 **represented by the error bars.**

242
 243 Average rates for NO₂⁻ reduction and N₂O production at pH 6.8 were calculated (Table 1). Rates were calculated per day and
 244 again these results emphasize that the amendment of dead biomass increased the rates by ~92%. Although not complete, Fe(II)
 245 oxidation in the presence of DB was also more pronounced leading to only 10.5 ± 2.8% Fe(II) remaining compared to the
 246 mineral-only setup in which 37.1 ± 8.2% Fe(II) remained. To complement the colorimetric data, ⁵⁷Fe Mössbauer spectroscopy
 247 was performed and data are presented in detail in the next section.

248
 249 **Table 1: Chemodenitrification kinetics and mineral transformation during mineral + dead biomass as well as the mineral only**
 250 **experiments. T_{ini} values represent means calculated by summarizing results across all pH ± standard error. Overall**
 251 **reduction/production rates are calculated by subtracting [C]_{t0} - [C]_{tend} ± standard error / [C]_{tend} - [C]_{t0} ± standard error,**
 252 **respectively and are given per day. Fe(III) values are calculated by using ⁵⁷Fe Mössbauer spectroscopy data. Mineral phases were**
 253 **also identified by using ⁵⁷Fe Mössbauer spectroscopy with spectra collected at 77 K. Mineral-only sample taken after 28 days was**
 254 **inadvertently destroyed prior to Mössbauer measurement.**

	Mineral + Dead Biomass	Mineral-only
NO ₂ ⁻ reduction (\bar{X})	0.053 ± 0.013 mmol L ⁻¹ day ⁻¹	0.004 ± 0.003 mmol L ⁻¹ day ⁻¹

N₂O production (\bar{X})	353.50 ±32.91 nmol L ⁻¹ day ⁻¹	204.02 ±60.29 nmol L ⁻¹ day ⁻¹
Fe(II)_{total} remaining (\bar{X})	10.54 ±2.77%	37.08 ±8.23%
Fe(III) after NO₂⁻ addition	7.4%	9.9%
Fe(III) after 28 days	48.7%	*
Mineral phase t_{ini}	Vivianite	Vivianite
Mineral phase t_{end}	Vivianite/Ferrihydrite	*

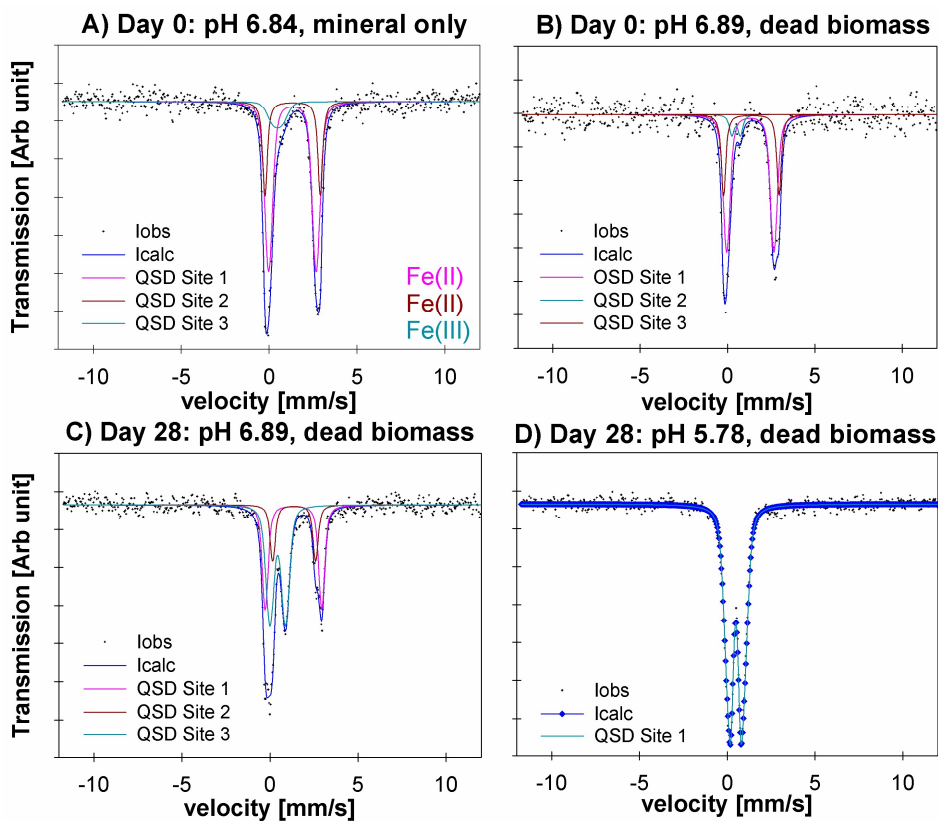
255 * Mössbauer sample ~~lost~~ *processing failed*

256

257 3.2. Fe mineral analysis

258 ⁵⁷Fe Mössbauer spectroscopy was used to quantify structural Fe(II) and Fe(III) contents of the samples and identify differences
259 in mineralogy under the different reaction conditions. The hyperfine parameters of the mineral phases in in the mineral-only
260 setup at t_{initial} (pH 6.84) are dominated by Fe(II) doublets (Figure 3 A, QSD Sites 1 and 2), which most closely match that of a
261 vivianite spectrum (Muehe et al., 2013; Veeramani et al., 2011). There is a small component with low centre shift and
262 quadrupole splitting, indicative of Fe(III), which accounts for ~10% of the spectral area (Figure 3 A, QSD Site 3). This suggests
263 some minor oxidation occurred, potentially during transfer of sample into the spectrometer. The mineral phases in the DB-
264 amended setup at t_{initial} (pH 6.89) shows very close approximation to the abiotic mineral-only setup, though with slightly less
265 Fe(III) (~7.5% of the spectral area) (Figure 3 B, QSD Site 2). Precipitates analysed at the end of the DB-amended experiment
266 (Day 28) show that at pH 6.89, the vivianite phase still dominates (Figure 3 C, QSD Sites 1 and 2), however, the Fe(III)
267 component is now much more prominent (Figure 3 C, QSD Site 3), and suggests the formation of a poorly crystalline/short-
268 ranged ordered mineral such as ferrihydrite (Cornell and Schwertmann, 2003). At the lowest pH (5.78) and in the presence of
269 DB, the pattern of the precipitates is completely dominated by one doublet (Figure 3 C, QSD Site 1), with hyperfine parameters
270 corresponding to a poorly ordered Fe(III) mineral such as ferrihydrite (Cornell and Schwertmann, 2003). Unfortunately, the
271 *sample processing failed for the* mineral-only sample taken after 28 days *was lost* and can therefore not be used for further
272 elucidations. Detailed fitting results of the ⁵⁷Fe Mössbauer spectroscopy are provided in Table 2.

273



274

275 Figure 3: ^{57}Fe Mössbauer spectra collected at 77 K for (A) the mineral only setup precipitates at day 0 and pH 6.84, (B) the mineral
 276 + dead biomass amended setup precipitates at day 0 at pH 6.89, (C) the mineral + dead biomass amended setup precipitates at day
 277 28 and (D) the mineral + dead biomass amended setup precipitates at day 28 at pH 5.78. Full lines represent the calculated spectra
 278 and their sums. Colours of the fits represent the corresponding Fe phase and thus vary between the graphs: Fe(II) doublets (A, C –
 279 QSD Sites 1 and 2, B – QSD Sites 1 and 3) closely match the spectra known for vivianite. Minor amounts of Fe(III) are present at
 280 day 0 in both, the mineral-only and DB-amended setups (A/B QSD Site 3/2). Single doublets shown in C (QSD Site 3) and D (QSD
 281 Site 1) correspond to a poorly ordered Fe(III) mineral such as ferrihydrite.

282

283

284

285

286 **Table 2: Fitting results of Mössbauer spectroscopy. CS – centre shift, QS – quadrupole splitting, R.A. – Relative abundance**
 287 **determined by integration under the curve, Chi² – goodness of fit; sample collection took place at t_{ini} – initial timepoint and t_{end} –**
 288 **end timepoint; MO = mineral-only, MDB = mineral + dead biomass.**

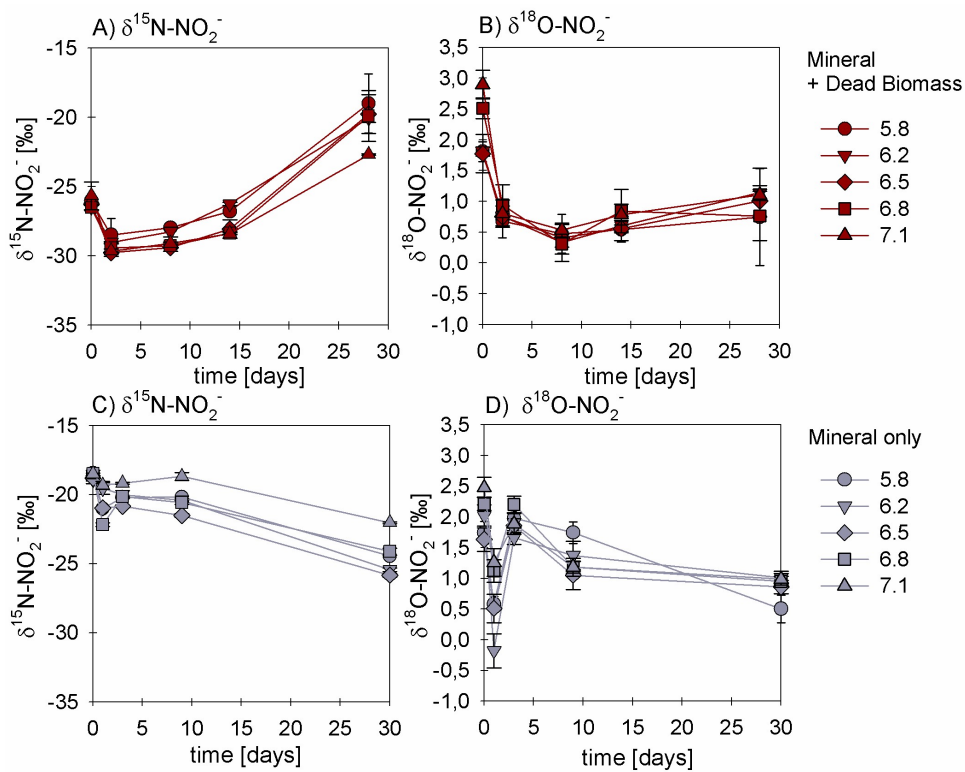
Sample	Temp [K]	Phase	CS [mm/s]	QS [mm/s]	R.A. [%]	Error	Chi ²
MO_pH6.8_t _{ini}	77	Fe(II)	1.32	2.71	66.0	23.0	0.55
		Fe(II)	1.33	3.15	24.0	23.0	
		Fe(III)	0.47	0.63	9.9	4.8	
MDB_pH6.8_t _{ini}	77	Fe(II)	1.30	2.70	65.0	14.0	0.68
		Fe(III)	0.49	0.49	7.4	3.6	
		Fe(II)	1.36	3.18	28.0	15.0	
MDB_pH6.8_t _{end}	77	Fe(II)	1.33	3.21	34.3	2.4	0.73
		Fe(II)	1.37	2.44	17.0	2.8	
		Fe(III)	0.44	0.89	48.7	2.4	
MDB_pH5.8_t _{end}	77	Fe(III)	0.49	0.79	100.0		0.66

289

290 3.3. Nitrite and N₂O isotope dynamics

291 In experiments with DB, the δ¹⁵N-NO₂⁻ and δ¹⁸O-NO₂⁻ values showed a very consistent initial ~3-4‰-decrease (from -26‰
 292 to -30‰ for δ¹⁵N and from ~+3‰ to 0‰ for δ¹⁸O) (Figure 4 A, B). After 5 days, the δ¹⁵N values started to increase again with
 293 decreasing NO₂⁻ concentrations, reaching final values of ~ -20‰ (Figure 4 A), whereas the concomitant increase in the δ¹⁸O-
 294 NO₂⁻ was much smaller (<1‰, Figure 4 B). The same pattern was observed for all pH levels. In mineral-only experiments,
 295 isotope trends were quite different. In combination with far less consumption of NO₂⁻, the δ¹⁵N-NO₂⁻ values decreased
 296 throughout the entire abiotic experiment (Figure 4 C). In contrast, the δ¹⁸O-NO₂⁻ first dropped by 2‰, reaching a clear
 297 minimum of ~-0.5 to -0.5 ‰, before rapidly increasing again. Over the remaining 25 days, the δ¹⁸O-NO₂⁻ slowly decreased
 298 reaching final values of ~-1‰ (Figure 4 D) – similar to that of the [mineral plus](#) DB treatment.

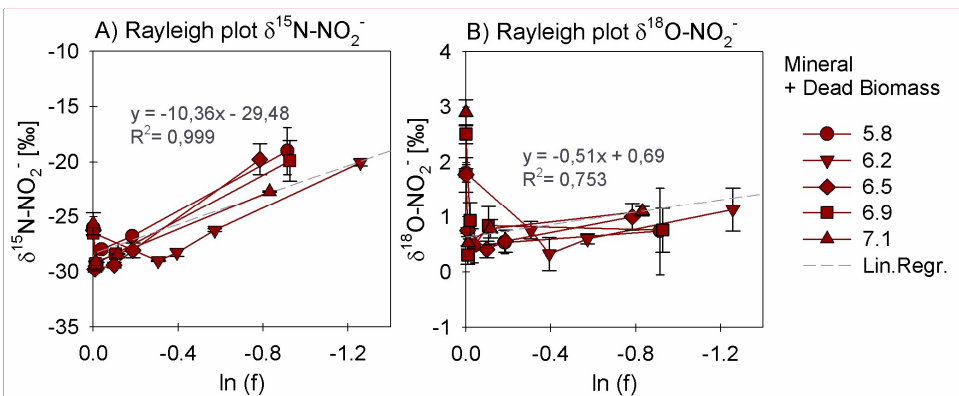
299



300
 301 **Figure 4:** $\delta^{15}\text{N}$ (A, C) and $\delta^{18}\text{O}$ (B, D) values for NO_2^- measured in the mineral + dead biomass amended (red) and the mineral-only
 302 (grey) setups over time and at different pH. Standard error calculated from biological replicates (n = 3) is represented by the error
 303 bars.

304
 305 In order to estimate the net N and O isotope fractionation for putative NO_2^- reduction (in the DB-amended experiments, where
 306 we observed a clear decrease in NO_2^-), we plotted the NO_2^- $\delta^{15}\text{N}$ and $\delta^{18}\text{O}$ values against the natural logarithm of the
 307 concentration of the residual NO_2^- (Rayleigh plot), where the slope of the regression line approximates the N and O isotope
 308 effects, respectively (Mariotti et al., 1981). At least after the initial period, when the NO_2^- $\delta^{15}\text{N}$ markedly increased with
 309 decreasing NO_2^- concentrations, the N isotope data are more or less consistent with Rayleigh isotope fractionation kinetics.
 310 The slope of the regression line suggests an average N isotope effect of -10.4‰ (Figure 5 A). For the mineral-only setup, no
 311 N isotope effect could be calculated, but the observed NO_2^- $\delta^{15}\text{N}$ trend suggest a small inverse N isotope fractionation (Figure

312 [4 C](#)). Similarly, trends in NO_2^- $\delta^{18}\text{O}$ of the DB experiments are not as obviously governed by normal Rayleigh fractionation
 313 dynamics, at least not during the initial period, when the $\delta^{18}\text{O}$ decreased despite decreasing NO_2^- concentrations. Considering
 314 the $\delta^{18}\text{O}$ values only after 2 days of the incubation, the Rayleigh plot revealed an average O isotope enrichment factor of -0.5
 315 ‰ (Figure 5 B), much lower than for N. Similar to N, O-isotope Rayleigh plots for the mineral-only experiments (Figure S54)
 316 did not exhibit coherent trends, as the fractional NO_2^- depletion was minor and not consistent (mostly less than 10%). Again,
 317 the observed $\delta^{18}\text{O}$ minimum at day 2 of the abiotic incubations suggests that processes other than normal kinetic fractionation
 318 during NO_2^- reduction were at work, which cannot be described with the Rayleigh model. If at all, the decreasing $\delta^{18}\text{O}$ values
 319 after day 5 in the mineral-only experiments, accompanying the subtle decrease in NO_2^- concentration in at least some of the
 320 treatments, suggest a small apparent inverse O isotope effect associated with the net consumption of NO_2^- . Despite the different
 321 NO_2^- $\delta^{18}\text{O}$ dynamics during the course of the experiment, the final $\delta^{18}\text{O}$ of the residual nitrite was very similar in both
 322 experimental setups, and independent of the pH.

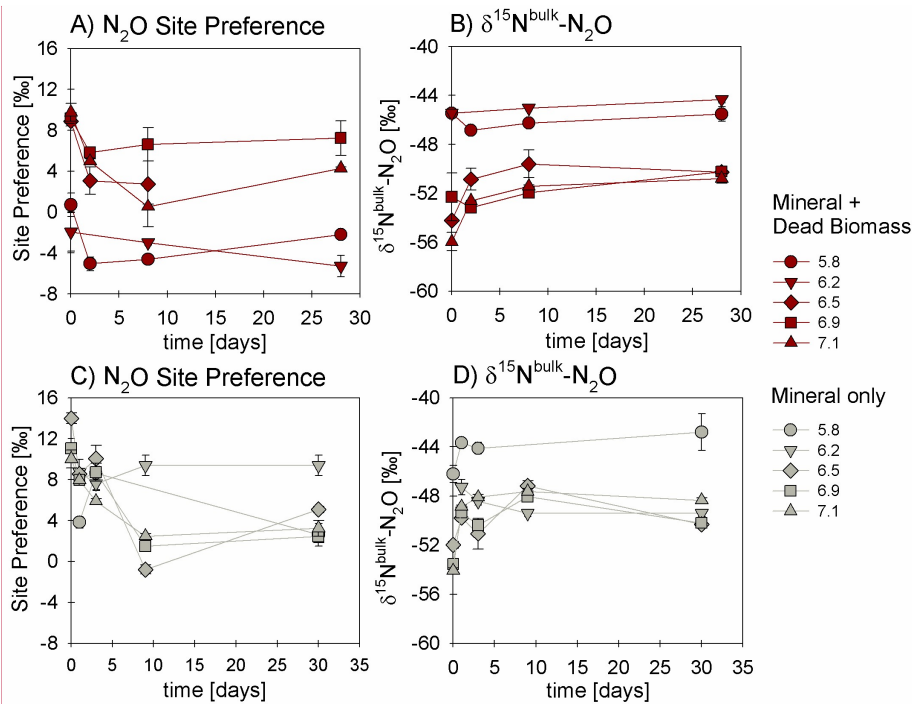


323
 324 **Figure 5:** Rayleigh plots for NO_2^- $\delta^{15}\text{N}$ (A) and $\delta^{18}\text{O}$ (B) values measured for the mineral + dead biomass amended setups over the
 325 \ln of the substrate fraction remaining and at different pH. The average linear regression line was calculated starting with the lowest
 326 delta values (after the initial decrease in both $\delta^{15}\text{N}$ and $\delta^{18}\text{O}$ during the initial experimental phase). Equation and R^2 are given in
 327 grey. Standard error calculated from biological replicates ($n = 3$) is represented by the error bars.

328
 329 We also investigated the N_2O isotope dynamics during mineral-only and **mineral plus DB DB-amended**-incubations. Site
 330 preference (SP) and $\delta^{15}\text{N}^{\text{bulk}}$ of the N_2O produced in both experimental setups were plotted over time (Figure 5-6 A and B) and
 331 show, except for a few values that require further investigation, almost no variation during the period of the experiment. Also,
 332 disregarding the rather high and unusual (but well replicated) values already mentioned, the majority of values obtained in
 333 both setups indicate that neither pH nor the amendment of DB seems to have had any influence on the isotopic composition of
 334 the produced N_2O (Figure 5-6 B vs. D). Over the course of the experiment, $\delta^{15}\text{N}^{\text{bulk}}$ N_2O values were around $-50 \pm 5\%$. SP

Kommentiert [AV3]: Changed title x-axis to $\ln(f)$

335 was relatively low, ranging roughly between -40 and a maximum of +140‰ (Figure 5-6 A, C), without any significant temporal
 336 change.



337
 338 **Figure 6: Site Preference (SP; A, C) and $\delta^{15}\text{N}^{\text{bulk}}$ (B, D) values of N_2O produced in experiments amended with mineral + dead biomass**
 339 **(red) and mineral-only (grey). For pH 6.5, the final SP value (A) is missing due to analytical problems (overly large sample peak**
 340 **areas in the raw data) which biased the results. Standard error calculated from biological replicates (n = 3 or 23; extreme values N**
 341 **= 2) is represented by the error bars.**

342
 343 Rayleigh diagrams, in which $\delta^{15}\text{N}^{\text{a}}$, $\delta^{15}\text{N}^{\text{bulk}}$ and SP of the N_2O were plotted against concentrations of the reactant (NO_2^-)
 344 remaining (Figure S6S5), confirm the similar N_2O isotope dynamics in the DB vs. mineral-only setups, despite the differential
 345 degree of NO_2^- reduction (only minor in the mineral-only experiment, with f always greater 0.9) and despite the different NO_2^-
 346 N and O isotope dynamics. Similarly, the dual N_2O $\delta^{18}\text{O}$ vs. $\delta^{15}\text{N}^{\text{bulk}}$ signatures (with the exception of two data points; Figure
 347 S6S7) were almost equivalent in both setups, implying that, although modes of NO_2^- reduction clearly differ, a similar
 348 mechanism of nitrite-reduction-associated N_2O production exists in both setups. The N and O isotopic results are summarized
 349 in Table 3 (see discussion).

Kommentiert [AV4]: Corrected graph

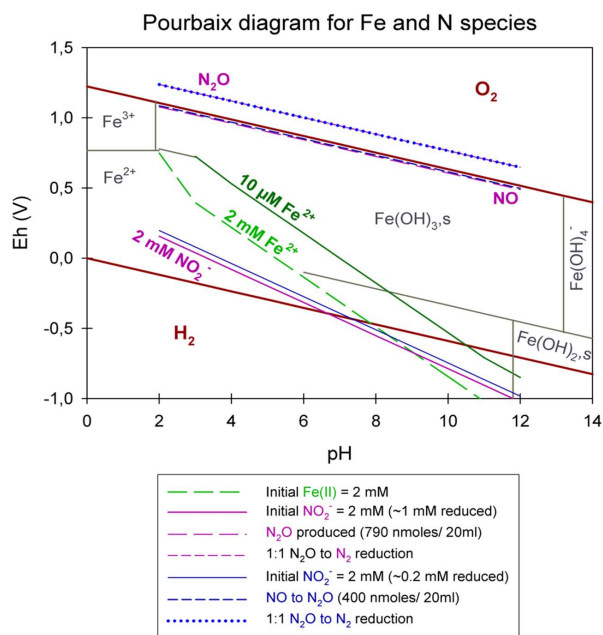
350 4. Discussion and implications

351 4.1. General evaluation of the abiotic reaction systematics

352 Overall, the abiotic reaction between NO_2^- and Fe(II), heterogenous or homogenous, has been considered thermodynamically
353 favourable, and as major contributor to the global N_2O budget (e.g. Jones et al., 2015; Otte et al., 2019). Previous studies on
354 abiotic NO_2^- reduction with Fe(II) have usually been performed in the presence of rather high concentrations (>2 mM) of NO_2^-
355 and/or Fe(II), without taking into account that chemodenitrification is in fact considered to be highly concentration-dependent
356 (Van Cleemput and Samater, 1995). In addition, reaction dynamics were often tested under variable conditions including the
357 presence of different Fe(II)/Fe(III) minerals, sediments, organic materials and/or bacterial cells (Chen et al., 2018; Grabb et
358 al., 2017; Otte et al., 2019). Whether NO_2^- indeed acts as a direct oxidant of Fe(II) at circumneutral pH or whether the reaction
359 requires catalysis is still a matter of debate (Kampschreur et al., 2011; Sorensen and Thorling, 1991).

360 Integrating concentrations that are pertinent to our experiments, we constructed a Pourbaix diagram (e.g. Delahay et al., 1950;
361 Minguzzi et al., 2012) (Figure 7). Based on these (simplified) thermodynamic calculations, the abiotic reaction solely driven
362 by the reaction of NO_2^- and aqueous Fe^{2+} at a pH range of 5 to 7 is not supported. Under our experimental conditions, Fe^{2+} is
363 predicted to be oxidized by NO rather than NO_2^- . Considering Figure 7, an accumulation of NO at μM or even mM
364 concentrations would result in a downward shift of the NO_2^- line. Therefore, an accumulation of NO would only lower the
365 reactivity between NO_2^- and Fe^{2+} , which implies that NO_2^- is not oxidizing Fe^{2+} . Again, this also implies that the reactivity
366 between NO_2^- and Fe^{2+} is only enhanced if NO concentrations are rather low (pM range). In order to avoid NO accumulation
367 and thus to enhance the abiotic reaction between NO_2^- and Fe^{2+} , NO would need to react further (either with Fe^{2+} or otherwise).
368 This would induce a reaction cascade, resulting in the constant reduction of NO_2^- and NO, and thus in higher N_2O
369 concentrations. In contrast, if NO does accumulate as previously reported, the reaction between NO_2^- and Fe^{2+} would be
370 suppressed and only NO could be reduced further to N_2O , a reaction that of course also depends on gas equilibration dynamics
371 occurring with the headspace of the system. Nevertheless, considering all these aspects, including the fact that the N_2O
372 produced corresponds only to a minor fraction of the initial NO_2^- reduced, NO acting as main oxidizing agent seems more
373 likely. The reaction mechanisms in this system are, however, complex and we note that this simplified thermodynamic analysis
374 does neglect catalytic effects that are possibly induced by reactive surfaces. The complexity of this system is further indicated
375 by the fact that, according to the Pourbaix diagram, a pH response towards N_2O accumulation would be expected which has,
376 however, never been reported so far. Furthermore, testing various pH did not reveal an obvious pH effect on the reaction
377 dynamics. Changes in pH will most certainly affect interactions between species such as HNO, NO_2 and N_2O and thus could
378 impact the reaction dynamics. **In addition, the results observed in the setup biased by accidentally adding twice as much NO_2^-**
379 **(DB, pH 5.8) do not differ from the results of the other setups and thus might question the previously mentioned concentration**
380 **dependency (i.e. $[\text{NO}_2^-]$).** It appears that, for a more detailed understanding of this redox system, the reactants/intermediates
381 involved and thus the specific reaction kinetics would need to be determined. Unfortunately, quantification of these
382 intermediates is hampered by their high reactivity, transient nature, and lack of detection techniques that can be applied in

383 batch culture experiments. Since low amounts (e.g., pM) of NO suffice to impact reaction dynamics and thus stimulate the
 384 reaction between NO_2^- and Fe^{2+} , NO quantification could be crucial to assess the environmental controls on Fe(II)-coupled
 385 chemodenitrification. In laboratory biological denitrification experiments, accumulation of NO has been reported (Goretski
 386 and Hollocher, 1988; Zumft, 1997) and was shown to even account for up to 40% of the initial NO_2^- amended (Baumgärtner
 387 and Conrad, 1992; Choi et al., 2006; Kampschreur et al., 2011; Ye et al., 1994; Zumft, 1997). Hence, Kampschreur et al.,
 388 (2011) concluded that chemodenitrification is not necessarily solely caused by a single-step reaction, and proposed that the
 389 oxidation of Fe^{2+} is rather caused by a two-step mechanism. They observed an immediate formation and accumulation of NO
 390 after NO_2^- was added to Fe^{2+} , and as soon as a considerable fraction of the Fe^{2+} was oxidized, N_2O formation was detected.
 391 Although NO and other possible intermediate (e.g. $\text{NO}_2(\text{g})$) concentrations might not play a major role with regard to mass
 392 balance considerations, their possible impact on the overall reaction systematics as well as the isotopic fractionation, remains
 393 unclear.



394
 395 **Figure 7:** Pourbaix diagram depicting an Fe and N-species based system. Overall calculations are based on the Nernst equation using
 396 values taken from literature (for equation and values see table S1). **Green lines** represent Fe^{2+} concentrations, **pink lines** represent
 397 NO_2^- reduction experiments, starting with 2 mM NO_2^- , resulting in the reduction of 1 mM NO_2^- , the production of 790 nmol /20 ml
 398 N_2O and a 1:1 transformation of N_2O to N_2 ; **blue lines** represent NO_2^- reduction experiments, starting with 2 mM NO_2^- , resulting
 399 in the reduction of 0.2 mM NO_2^- , the production of 790 nmol /20 ml N_2O and a 1:1 transformation of N_2O to N_2 . Reduction/production
 400 values were taken from our results presented in 3.1.

401 4.2. Surface catalysis of chemodenitrification

402 Previous studies have shown that the initial presence of either Fe(III)(oxyhydr)oxides (Coby & Picardal, 2005; Klueglein &
403 Kappler, 2013; Sorensen & Thorling, 1991) or amorphous Fe(II) minerals (Van Cleemput and Samater, 1995) can stimulate
404 the abiotic reaction between NO_2^- and Fe^{2+} . As summarized in Table 1, under mineral-only conditions NO_2^- reduction was
405 significantly lower ($0.004 \pm 0.003 \text{ mmol L}^{-1} \text{ day}^{-1}$) than in identical experiments containing DB, which substantially enhanced
406 NO_2^- reduction ($0.053 \pm 0.013 \text{ mmol L}^{-1} \text{ day}^{-1}$). The catalytic effect of Fe minerals on the abiotic NO_2^- reduction, which has
407 been demonstrated before, seems to be amplified in the presence of DB. Relative to NO_2^- reduction rates, overall final N_2O
408 yields per mole NO_2^- reduced tended to be higher in the mineral-only setups. However, considering the initial NO_2^-
409 concentrations, only minor amounts of N_2O were produced in both setups, raising questions about the contribution of
410 chemodenitrification to global N_2O emissions discussed by others (Grabb et al., 2017; Jones et al., 2015; Otte et al., 2019;
411 Zhu-Barker et al., 2015). For example, in comparison to the N_2O yields in experiments where chemodenitrification was
412 catalysed by green rust (up to 31%, Grabb et al., 2017), the amount of N_2O produced in our setups is far lower (<5% of the
413 initial NO_2^-).

414 Fe-bearing minerals are known for their high reactivity, ability to complex ligands (metals, humics) and phosphates, and
415 surface protonation capacity via the sorption of OH⁻ groups (Elsner et al., 2004; Stumm and Sulzberger, 1992). Surface
416 catalytic effects may include *direct* and *indirect* sorption-induced catalysis. In the environment, pH has been shown to have a
417 strong influence on these sorption capacities of Fe minerals in general (Fowle and Konhauser, 2011). Considering the point of
418 zero charge (PZC) of vivianite, which is with 3.3 below the lowest tested pH in our experiments, the mineral surface is
419 positively charged under our experimental conditions (Luna-Zaragoza et al., 2009). Hence the pH range tested here will not
420 affect the surface charge, and NO_2^- sorption onto mineral surfaces and corresponding heterogeneous reactions are possible. In
421 contrast, cell surfaces are considered to be negatively charged (Wilson et al., 2001) and therefore might induce different effects
422 than mineral surfaces. The charge of the cell surface most likely remained negative even after autoclaving (see e.g. Halder et
423 al., 2015). Our results imply that the systematics of chemodenitrification are strongly dependent on the surface provided and
424 that, depending on the availability and quality of catalytic surfaces, Fe coupled chemodenitrification may be a single-step
425 reaction (between NO_2^- and Fe) or may occur in multiple steps (reaction between Fe and NO_2^- , as well as Fe and NO). As a
426 consequence, the nature of surface catalysis would likely have a strong impact on the N_2O yield per mole NO_2^- reduced to NO.
427 Since NO has been demonstrated to have a ~~strong rather exceptional~~ affinity towards Fe^{2+} and Fe^{3+} centres resulting in the
428 formation of $\text{Fe}^{\text{x+}}(\text{NO})_n$ nitrosyls and thus triggering an enhancement of the N_2O decomposition rate (e.g. Rivallan et al., 2009).
429 It remains unclear to what extent, and why, the quality of the catalytic surfaces plays a role. Particularly in the presence of
430 organics and/or dead bacterial cells, which are known to have a high affinity to bind metal ions (e.g. Ni^{2+} , Cu^{2+} or Zn^{2+}), either
431 directly or by forming surface complexes with hydroxyl groups (Fowle and Konhauser, 2011), a surface-catalysis-induced
432 reaction can be expected. Besides acting as a catalyst via a reactive surface, the dead biomass might also have directly triggered
433 the reaction. For example, non-enzymatic NO formation was studied and modelled by Zweier et al. (1999), suggesting that at

434 concentrations between 100 and 1000 μM , abiotic NO_2^- disproportionation and thus NO formation at circumneutral pH in
435 organic tissue is still possible (Zweier et al., 1999). Furthermore, autoclaving might have ruptured cell walls and released
436 organic compounds. In the presence of phenolic compounds, humic substances, and other organic compounds, NO_2^- has been
437 shown to form NO via self-decomposition (Nelson and Bremner, 1969; Stevenson et al., 1970; Tiso and Schechter, 2015).
438 Whether this may have been the case also in our experiments remains unclear, since we did not conduct experiments containing
439 only DB and NO_2^- . Another possible consideration is the presence of extracellular polymeric substances (EPS), which should
440 also be tested in future studies. Liu et al., (2018) investigated nitrate-dependent Fe(II) oxidation with *Acidovorax* sp. strain
441 BoFeN1, showing that *c*-cytochromes were present in EPS secreted which could indeed act as electron shuttling agents
442 involved in electron transfer supporting chemolithotrophic growth. Since *S. oneidensis*, our model organisms used as DB
443 supply, is known to produce large amounts of EPS, harbouring *c*-cytochromes (Dai et al., 2016; Liu et al., 2012; White et al.,
444 2016), a potential impact of EPS on the reaction between NO_2^- and Fe(II) needs to be considered. However, possible
445 cytochromes present in the EPS most likely lost their activity due to protein denaturation during autoclaving (Liu &
446 Konermann, 2009; Tanford, 1970). Nevertheless, EPS is still present and can act as a catalysing agent to the abiotic reaction
447 mechanism (Klueglein et al., 2014; Nordhoff et al., 2017).
448 Fe(II)_{total} oxidation via NO_2^- has also been observed in the mineral-only setups, but to a lower extent. Hence, the vivianite
449 mineral surfaces themselves seem to catalyse the abiotic reaction between NO_2^- and Fe(II)/ Fe^{2+} (in parts, the stimulation of
450 Fe-dependent nitrite reduction may also be attributed vivianite dissolution providing ample Fe(II) substrate). Previous studies
451 reported on mineral-enhanced chemodenitrification (Dhakal et al., 2013; Grabb et al., 2017; Klueglein & Kappler, 2013;
452 Rakshit et al., 2008), and the catalytic effect may be due to NO_2^- adsorption onto the minerals surface possibly facilitating a
453 direct electron transfer. Similar findings have been reported previously on Fe(II) oxidation promoted by electron transfer
454 during adsorption onto a Fe(III) minerals surface (Gorski and Scherer, 2011; Piasecki et al., 2019). OH^- adsorption is probably
455 enabled by the minerals positive surface charge at pH >6, resulting in a limited reactive surface availability. Complexation of
456 dissolved Fe^{2+} , which is provided by mineral dissolution, by OH^- groups would thus result in a lower overall NO_2^- reduction
457 rate compared to the DB-amended setups. Nevertheless, the NO formed by the initial NO_2^- reduction could, at still elevated
458 Fe^{2+} levels, proceed until both dissolved and adsorbed Fe(II) is quantitatively oxidized to surface-bound Fe(III) (Kampschreur
459 et al., 2011). This would ultimately lead to similar Fe(II)_{total} oxidation and N_2O production (and thus higher N_2O yields) as in
460 the DB amended experiment and thus explain the similar results.

461 4.3. Mineral alteration during Fe-coupled chemodenitrification

462 We used ^{57}Fe Mössbauer spectroscopy in order to determine, whether the catalytic effects that enhanced chemodenitrification
463 with Fe^{2+} also modulated mineral formation. In both setups, addition of Fe(II)Cl_2 to the 22 mM bicarbonate buffered medium
464 led to the formation of vivianite, an Fe(II)-phosphate. Shortly after the addition of $\text{Fe}^{2+}_{\text{aq}}$, the mineral phase in both setups was
465 dominated by Fe(II), but a small fraction of Fe(III) was also present. Initial fractions of Fe(III) were similar in both the mineral-
466 only and DB-amended experiments (9.9% and 7.4%, respectively) and, if not an artefact of Mössbauer sample handling, might

467 therefore have stimulated Fe(II) adsorption and oxidation (Gorski and Scherer, 2011; Piasecki et al., 2019). The reduction of
468 NO_2^- was accompanied by a marked increase of Fe(III), likely in the form of short-range ordered ferrihydrite or lepidocrocite.
469 Thus, the Fe(III) phase detected at day 0 most likely formed immediately after NO_2^- addition. This is supported by prior studies,
470 which demonstrated the initiation of Fe(II) oxidation with NO_2^- within a short period of time (Jamieson et al., 2018; Jones et
471 al., 2015). At the end of the DB experiment at pH 6.89, oxidized Fe(III) (most likely in the form of poorly ordered ferrihydrite)
472 contributed 48.7% to the total Fe phases, with vivianite accounting for the remaining spectral area. Unfortunately, we are
473 unable to compare the results of the DB-amended precipitates at the end of the experiment to the mineral-only setup, since the
474 sample was lost/processing failed. In contrast to our observations, other studies conducted in the presence of organics have
475 identified goethite as the main Fe(III) phase during the abiotic reaction between Fe(II) and NO_2^- (Chen et al., 2018; Liu et al.,
476 2018). In NDFeO experiments, the formation of lepidocrocite, goethite, hematite and to some extent, magnetite has been
477 reported. Minerals obtained from the enrichment culture KS were mostly vivianite and ferrihydrite, which is, however,
478 attributed to the fact that for the cultivation of the KS culture a high-phosphate medium is used (Nordhoff et al., 2017). In the
479 abiotic experiments (10 mM Fe(II) and 10 mM NO_2^-) presented by Jones et al., (2015), the formation of lepidocrocite, goethite
480 and two-line ferrihydrite were observed after 6 to 48 hrs. In the experiments presented here, besides a short-range ordered
481 Fe(III) phase, likely ferrihydrite, no other mineral phases could be identified after 28 days.
482 Iron analysis also indicates that the oxidation of the $\text{Fe(II)}_{\text{total}}$ went to completion at pH 5.8 whereas at pH 6.8, 52.3% of the
483 $\text{Fe(II)}_{\text{total}}$ remained at the end of the incubation experiment, resulting in the formation of a poorly-ordered ferrihydrite.
484 Unfortunately, we did not measure the zeta potential of the starting solutions, which would probably help to explain the
485 differences detected. We note that, although ^{57}Fe Mössbauer spectroscopy was used to measure the Fe(II)/Fe(III) in the
486 precipitates, the reported $\text{Fe(II)}_{\text{total}}$ concentrations reflect the total Fe(II), i.e., of both the dissolved pellet (structurally-bound
487 or adsorbed) and the aqueous Fe^{2+} in the supernatant measured by Ferrozine. The results obtained by Mössbauer analysis (50%
488 Fe(II) remaining) seem to contradict the ferrozine assay (<10% remaining) (see Table 1 and 2). The presence of ferrous Fe,
489 either as structurally-bound Fe(II) or adsorbed Fe^{2+} does indeed play a crucial role with regards to the reaction dynamics
490 occurring at the mineral surfaces, particularly if we assume that N-reactive species are also still present (Rivallan et al., 2009).
491 In addition, the initially formed Fe(III) phase might also induce another feedback to the N and even the Fe cycle since Fe(III)
492 minerals are also highly reactive (Grabbe et al., 2017; Jones et al., 2015). Mineral structure and thus Fe(II) location within the
493 lattice can influence the overall Fe accessibility, the binding site at the mineral surface and thus overall reactivity (Cornell and
494 Schwertmann, 2003; Luan et al., 2015; Schaefer, 2010). If the initial formation of Fe(III), however, enhanced the reaction
495 between NO_2^- and Fe(II), similar results in both setups should have been observed, which this was not the case since NO_2^-
496 reduction patterns in the mineral-only experiments were much lower. This also indicates again, that the presence of DB indeed
497 contributed greatly to the reaction in the DB experiments. Furthermore, results obtained from Mössbauer analysis are the only
498 results supporting a pH-dependent effect: At pH 5.78 and in the presence of DB, all vivianite was fully transformed into a
499 short-range ordered Fe(III) phase whereas at pH 6.89, vivianite remained a major component. This presence of vivianite also
500 indicates that no further Fe(II) oxidation occurred even though NO_2^- reduction was incomplete. The incomplete reduction of

501 NO₂⁻ in turn suggests that further Fe(II) oxidation was limited due to blocked or deactivated reaction sites on mineral surfaces.
502 Also, considering that at pH 5.8 and in the presence of DB, the initial NO₂⁻ concentrations were higher but the overall reaction
503 dynamics were quite similar to the other reaction conditions, the concentration dependency of the reaction between NO₂⁻ and
504 Fe(II) is again supported.

505 4.4. Nitrite and N₂O N and O isotope dynamics during chemodenitrification

506 In the presence of only vivianite, a decrease in δ¹⁵N-NO₂⁻ of ~3‰ ~~was observed with the initial decrease occurred in parallel~~
507 ~~with initially decreasing in~~ NO₂⁻ concentrations. Initial δ¹⁸O-NO₂⁻ values also reflect this drop of 3‰ during the first 3 days
508 but level off and stabilize at 1‰ after 9 days. The initial decrease in both δ¹⁵N and δ¹⁸O of NO₂⁻ suggest apparent inverse
509 isotope effects, which to the best of our knowledge have never been observed during chemodenitrification, and have only been
510 reported for enzymatic NO₂⁻ oxidation (Casciotti, 2009). Since biological NO₂⁻ oxidation can be ruled out (no NO₃⁻ produced,
511 no microbes), the decrease in δ¹⁵N-NO₂⁻, though subtle, could indicate that either heavy isotopes are incorporated in the
512 products formed (i.e. NO, N₂O), at least at the beginning of the incubation period. Normally, the heavier isotopes build
513 compounds with molecules of higher stability (Elsner, 2010; Fry, 2006; Ostrom & Ostrom, 2011). This is particularly true for
514 the formation of some minerals or highly stable molecules that are formed under mineral-only conditions, where processes can
515 reach an isotopic equilibrium (He et al., 2016; Hunkeler & Elsner, 2009; Li et al., 2011; Ostrom & Ostrom, 2011). However,
516 in the system presented here, N incorporation into mineral phases can be excluded, hence another process must favour the
517 heavy N-atoms. Since this initial drop in δ¹⁵N was also observed in the DB-amended experiments, a possible explanation might
518 be that the isotope values here reflect the sorption or complexation mechanism of NO₂⁻ onto the reactive surfaces. In contrast
519 δ¹⁸O-NO₂⁻ values, after the initial decrease, did not change greatly with decreasing NO₂⁻ concentrations. The stabilization of
520 the δ¹⁸O-NO₂⁻ towards the end of the experiment most likely reflects the oxygen isotope equilibration between δ¹⁸O-NO₂⁻ and
521 the δ¹⁸O of the water in the medium. Temporal δ¹⁸O-NO₂⁻ dynamics did not change greatly between the different pH treatments,
522 and in all cases the final δ¹⁸O-NO₂⁻ ranged between 0.5 and 1‰. The kinetics of abiotic O-atom exchange is a function of
523 temperature and pH. At near neutral pH, at room temperature, one can expect NO₂⁻ to be fully equilibrated after two to three
524 days (Casciotti et al., 2007). At higher pH, the first order rate constants for the equilibration with water are lower (Buchwald
525 and Casciotti, 2013), but equilibrium conditions should have been reached well within the incubation period. Indeed, the final
526 δ¹⁸O-NO₂⁻ was consistent with an equilibrium O isotope effect between NO₂⁻ and H₂O with a δ¹⁸O of ~-11.5‰ (Buchwald and
527 Casciotti, 2013). With regards to δ¹⁵N-NO₂⁻ values of the DB-amended experiments, a similar behaviour is found within the
528 first 3 days (i.e., decrease in δ¹⁵N), followed by a clear increase in δ¹⁵N-NO₂⁻ of ~10%. While it is difficult to explain the
529 initial decrease in δ¹⁵N-NO₂⁻ (a feature that was not observed in other chemodenitrification experiments (i.e. Grabb et al., 2017;
530 Jones et al., 2015), the subsequent increase in δ¹⁵N can be attributed to normal isotopic fractionation associated with
531 chemodenitrification and an N isotope effect (-9‰) that is consistent with those previously reported on Rayleigh-type N and
532 O isotope kinetics during chemodenitrification with Fe(III)-bearing minerals such as nontronite and green rust (Grabb et al.,
533 2017). In contrast, δ¹⁸O-NO₂⁻ values initially decrease as in the abiotic experiment but then level off faster reaching final values

534 of ~1‰, again most likely explained by O atom isotope exchange pulling the $\delta^{18}\text{O}\text{-NO}_2^-$ values towards the O-isotope
535 equilibrium value. This value is given by the $\delta^{18}\text{O}_{\text{H}_2\text{O}} + {}^{18}\epsilon_{\text{eq,NO}_2^-}$, whereas the latter is defined as the equilibrium isotope effect
536 between NO_2^- and H_2O and has been shown to yield values of roughly +13‰ (Casciotti et al., 2007). Overall, it seems that the
537 non-linear behaviour of the NO_2^- in the O isotope Rayleigh plot is most likely due to the combined effects of kinetic O isotope
538 fractionation during NO_2^- reduction, and O atom exchange between NO_2^- and H_2O .

539 NO_2^- N and O isotope trends observed under the DB-amended conditions (in which a large portion of the NO_2^- pool was
540 consumed), somewhat contradict prior reports of chemodenitrification exhibiting a clear increase in both $\delta^{15}\text{N}$ and $\delta^{18}\text{O}\text{-NO}_2^-$,
541 with N isotope enrichment factors for NO_2^- reduction between -12.9 and -18.1‰ and an O isotope effect of -9.8‰ (Jones et
542 al., 2015). Consistent with our data, however, they also observed that, at least in abiotic experiments where NO_2^- consumption
543 is rather sluggish due to Fe^{2+} limitation (as a result of either oxidation or simply occlusion), O-isotope exchange isotope effects
544 mask the effects of kinetic O isotope fractionation. While we cannot say at this point what exactly governs the combined NO_2^-
545 N vs. O isotope trends in the two different experimental conditions, we observed that the two processes (water isotope
546 equilibrium and KIE) competing with each other lead to different net dual isotope effects. Our data cannot resolve whether
547 these observations reflect fundamental differences or simply changes in the relative proportion of the competing processes.
548 Nevertheless, our observations may still be diagnostic for chemodenitrification catalysed by a mineral surface on the one hand,
549 and Fe-coupled chemodenitrification that involves catalytic effects by dead bacterial cells on the other. The mineral catalyst
550 evidently plays an important role with regards to chemodenitrification kinetics, reaction conditions, surface complexation or
551 contact time between the NO_2^- substrate and the mineral phase (Samarkin et al., 2010), and in turn the combined
552 kinetic/equilibrium N and O isotope effects.

553 The $\Delta^{15}\text{N}$ values ($\Delta^{15}\text{N} = \delta^{15}\text{N}_{\text{nitrite}} - \delta^{15}\text{N}_{\text{N}_2\text{O}^{\text{bulk}}}$) presented in Table 3 were obtained by subtracting the average $\delta^{15}\text{N}^{\text{bulk}}$ value of
554 N_2O (abiotic $-496.5 \pm 0.26\text{‰}$; dead biomass $-50.549.4 \pm 1.0.8\text{‰}$) across all pH and throughout the experiment from the average
555 of the initial $\delta^{15}\text{N}_{\text{nitrite}}$ value. These values can provide insight on reaction kinetics between NO_2^- , NO , and N_2O (Jones et al.,
556 2015). In both setups there is an offset between the NO_2^- and N_2O $\delta^{15}\text{N}$, which is clearly higher than what would be expected
557 based on the NO_2^- reduction NO_2^- isotope effect of <10‰. Following the argumentation of Jones et al. (2015), who reported a
558 similar N isotopic offset between NO_2^- and N_2O of $27.0 \pm 4.5\text{‰}$, this could be indicative for a heavy N accumulating in a
559 forming NO pool, whereas ^{14}N is preferentially reacting to N_2O or N_2 , respectively. This might even be supported by the rather
560 low $\delta^{15}\text{N}^{\text{bulk}}$ values detected for N_2O in both setups.

561
562
563
564
565

566 **Table 3: Comparison of the isotope values obtained during dead biomass versus the abiotic experiments. T0 values represent means**
567 **calculated by summarizing results across all pH \pm standard error. $\delta^{15}\text{N}$ and $\delta^{18}\text{O}$ values were calculated using $\bar{x}_{t0} - \bar{x}_{tend}$, whereas**

Kommentiert [ML5]: Make sure the table is not split over two different pages

568 **an overall increase from the initial value is marked with ↑, and a decrease with ↓. The calculated isotope fractionation factor (ε)**
 569 **was calculated** is based on the slope between the lowest initial value (here at t_i) and t_{end} for all pH. Δ¹⁵N (= δ¹⁵N_{nitrite} - δ¹⁵N_{2O^{bulk}}) was
 570 calculated for the end of the experiment.

	Dead Biomass	Abiotic
δ ¹⁵ N _{nitrite(t₀-t_{end})}	↑5.99 ±0.65‰	↓5.93 ±0.73‰
δ ¹⁸ O _{nitrite(t₀-t_{end})}	↓1.75 ±0.23‰	↓1.15 ±0.18‰
¹⁵ ε _{nitrite}	-10.36 ‰ [#]	-
¹⁸ ε _{nitrite}	-0.51‰ [#]	-
SP	2.31 ↑1.7 ±1.2‰	6.55 ↓9.99 ±0.84‰
δ ¹⁵ N ^a	-48.95 ↑1.84 ±0.1‰	-46.34 ↓3.53 ±0.046‰
δ ¹⁵ N _{bulk}	-49.38 50.5 ±1.04 0.8‰	-46.48 49.5 ±2.10.6‰
Δ ¹⁵ N	24.42 3.2‰	30.92 7.85‰

571 [#] n=4 (t₁ to t_{end}); - concentrations in abiotic experiment fluctuate and show only minor decrease, hence ¹⁵ε and ¹⁸ε could not be calculated.
 572

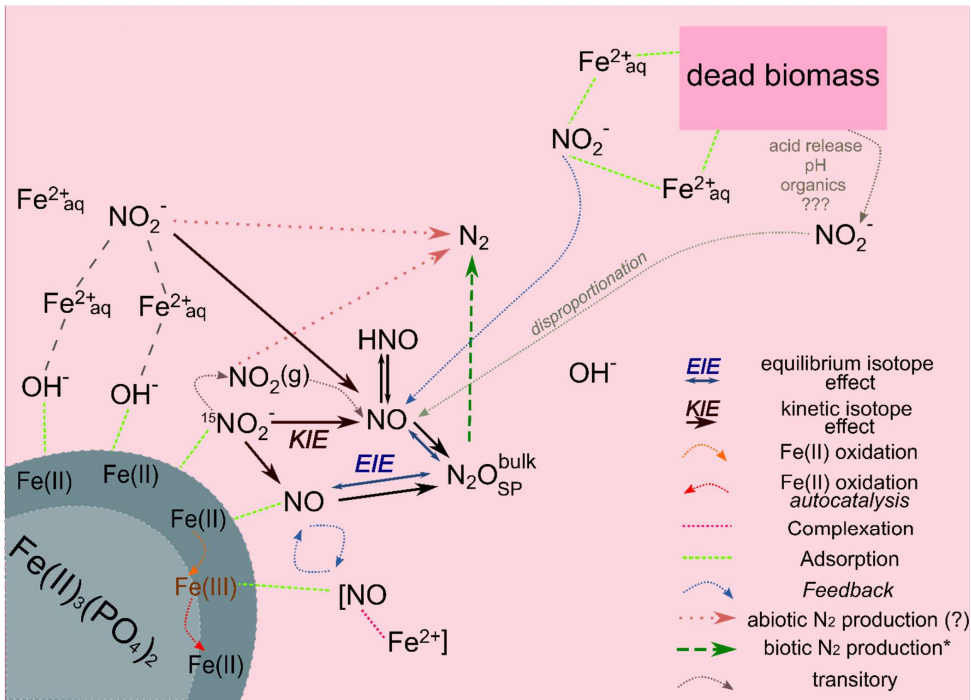
573 While our results clearly showed that N₂O accumulates over the course of the reaction, it remains unclear, which additional
 574 end products are present at the final stage of the experiment. If NO accumulates (instead of following the reaction cascade
 575 further), the substrate-product relationship between the δ¹⁵N-NO₂⁻ and δ¹⁵N-N₂O values that would be expected in a closed
 576 system is perturbed, leading to significantly higher Δ¹⁵N than predicted by the δ¹⁵N-NO₂⁻ trend. Hence, the calculated Δ¹⁵N of
 577 the mineral-only treatment (30.927.9‰) is **only** slightly higher than that of the DB experiment (24.423.2‰), and would
 578 therefore suggest that despite the differences in chemodenitrification kinetics (i.e., different NO₂⁻ reduction rates and extent),
 579 the NO pool formed is enriched in heavy N in both treatments, respectively. Alternatively, fractional reduction of the produced
 580 N₂O to N₂ may also affect the Δ¹⁵N since it would presumably increase the δ¹⁵N-N₂O and thereby raise the low δ¹⁵N-N₂O
 581 closer to the starting δ¹⁵N-NO₂⁻. Abiotic decomposition of N₂O to N₂ in the presence of Fe-bearing zeolites has been
 582 investigated previously (Rivallan et al., 2009), however, it remains unclear if this process could also occur here. Fractional
 583 N₂O reduction is also not explicitly indicated by the SP values, which would reflect an increase with N₂O reduction (Ostrom
 584 et al., 2007; Winther et al., 2018). The SP values in both mineral-only and DB-amended experiments were, with some
 585 exceptions, relatively low (6.50 ± 0.8‰; ~~2.31~~↑1.7 ± 1.2‰; Fig. 6, Table 3). In fact, SP values observed during the course of our
 586 experiments are significantly lower compared to SP values reported in other studies on Fe-oxide-mineral associated
 587 chemodenitrification (e.g., ~16‰; Jones et al. (2015); 26.5‰; Grabb et al. 2017), or during the abiotic N₂O production during
 588 the reaction of Fe and a NH₂OH/NO₂⁻ mixture (34‰; Heil et al. 2014). While the variety of different SP values for
 589 chemodenitrification-derived N₂O suggests different reaction conditions and catalytic effects, our SP data seem to imply that
 590 the mineral catalyst plays only a minor role with regards to the isotopic composition of the N₂O produced. However, since
 591 N₂O concentrations, even if minor, are increasing towards the end of the experiments, production and possible decomposition
 592 as well as ongoing sorption mechanisms might also serve as possible explanation leading to these rather low SP values. N₂O

593 SP values have been used as valuable tracer for microbial N₂O production (Ostrom & Ostrom, 2012). Based on pure culture
594 studies (Ostrom et al., 2007; Winther et al., 2018; Wunderlin et al., 2013) and investigations in natural environments (Wenk
595 et al., 2016) a SP range of -10 to 0‰ is considered to be characteristic for denitrification or nitrifier denitrification (Sutka et
596 al., 2006; Toyoda et al., 2005), whereas higher values are usually attributed to nitrification or fungal denitrification (Ostrom
597 & Ostrom, 2012; Wankel et al., 2017; Well & Flessa, 2009). The SP values reported here (0 to 140‰) fall well within the
598 range of biological N₂O production, explicitly denitrification and soil derived denitrification (2.3 to 16‰) (Ostrom & Ostrom,
599 2012), rendering the separation between chemodenitrification and microbial denitrification based on N₂O isotope
600 measurements difficult, if not impossible.

601 In summary, the N and O isotope systematics of chemodenitrification are multifaceted, depending on the environmental
602 conditions, reaction partners provided, and/or the speciation of precipitated mineral phases. The systematics observed here are
603 clearly not entirely governed by normal kinetic isotope fractionation only, as has also been observed in previous work. Grabb
604 et al. (2017) demonstrated that there is a relationship between reaction rate and kinetic NO₂⁻ N and O isotope effects, with
605 faster reaction leading to lower ¹⁵ε and ¹⁸ε. Again, changes in the expression and even in the direction of the isotope effects in
606 the NO₂⁻ pool suggest that multiple processes, including equilibrium isotope exchange (at least with regards to the δ¹⁸O- NO₂⁻
607), are contributing to the net N and O isotope fractionation regulated by the experimental conditions and reaction rates. As
608 pointed out by Grabb et al. (2017), and as supported by our comparative study with pure abiotic mineral phases and with added
609 dead biomass, the accessibility of Fe(II) to the reaction may be a key factor regarding the degree of N and O isotope
610 fractionation expressed, particularly if complexation limits the reactive sites of the mineral. The conditions that, at least
611 transiently, lead to the apparent inverse N and O isotope fractionation observed here for chemodenitrification requires
612 particular attention by future work. At this point, we can only speculate about potential mechanisms, which are indicated in
613 the conceptual illustration (Figure 8). As chemodenitrification seems to be catalysed by reactive surfaces of Fe(II)/Fe(III)-
614 minerals and/or organics (including cells), sorption onto these surfaces might play a crucial role in the fractionation of N and
615 O isotopes. For example, during the catalytic hydrogenation of CO₂ on Fe and Co catalysts, a subtle depletion (ca. 4‰) in
616 ¹³C at progressed conversion to methane has been explained by the precipitation of a ¹³C-enriched carbon intermediate (e.g.,
617 CO-graphite) on the catalyst surface (Taran et al., 2010). We are fully aware that it is difficult to compare our system with
618 Fischer-Tropsch synthesis of methane occurring at high temperature and pressure. Yet given the indirect evidence for NO
619 accumulation in our experiments, it may well be that preferential chemisorption/complexation of “heavy” intermediate NO
620 occurs, which may lead to transient ¹⁵N-depletion in the reactant NO₂⁻ pool. Considering that the N₂O concentrations measured
621 in our experiments were comparatively low and that δ¹⁵N^{bulk} N₂O values did not noticeably change throughout the experiments,
622 it is unlikely that N₂O is the final product, and formation of N₂ via abiotic interactions between NO₂⁻ and NO may is probably
623 also be involved (Doane, 2017; Phillips et al., 2016). Considering the accumulated product equation (see e.g. Casciotti et al.,
624 2011) and estimate of the δ¹⁵N^{bulk} value of N₂O, although N₂O is clearly not the only product here, can at least be calculated
625 for the mineral plus DB amended setups. The calculated Indeed, if accumulated as final product, the δ¹⁵N^{bulk}-N₂O value at
626 the end of the incubation should be therefore yield ~-332.9‰ (according closed-system accumulated-product Rayleigh

Kommentiert [AV6]: Used:
 $D^{15}N_{pA} = d^{15}N_{s,0} - 15e^*f \ln(f)/(1-f)$
See
https://www.who.edu/cms/files/jhayes/2005/9/IsoCalcs30Sept04_5183.pdf
Equation 46
Or Casciotti 2011 Equation 11.3

627 dynamics), which is roughly 10% higher than what we have measured (~ -50 ± 6 ‰).
 628 Unfortunately, due to the branching effect occurring during reduction (i.e. O atoms get plucked off and lost along the reaction),
 629 this estimation cannot be performed for the $\delta^{18}\text{O}-\text{N}_2\text{O}$ values. Hence, considering all these attempts to understand this complex
 630 system, it becomes very clear that N_2O is likely to be indeed meddling with the overall reaction dynamics either as an
 631 intermediate or as a side product, and can thereby influence the overall N and O isotope dynamics in highly complex ways.



632
 633 Figure 8: Conceptual figure depicting the proposed reaction mechanisms and feedbacks between the different N species during
 634 chemodenitrification induced by the presence of a mineral surface (lower left corner) or (dead) biomass (upper right corner).
 635 Adsorption of Fe^{2+} (directly or via complexation by OH^-) as well as NO_2^- could catalyse a direct reaction between both. In addition,
 636 NO_2^- adsorption onto the Fe(II) mineral might also induce disproportionation, leading to NO_x formation. These formed
 637 intermediates, although transitory, may impact the overall reaction dynamics by e.g. complex formation (i.e. $[\text{NO}-\text{Fe}^{2+}]$) or direct
 638 Fe(II) oxidation. The produced Fe(III) might induce another feedback loop (autocatalysis) resulting in further Fe(II) oxidation.
 639 Similar processes are possibly induced by the presence of (dead) biomass. Adsorption and complexation of either NO_2^- and Fe^{2+}
 640 would enhance the reaction between both. In addition, the presence of organic acids would decrease the pH locally and thereby
 641 promote and accelerate NO_2^- disproportionation and thus additionally enhance Fe(II) oxidation. Our results suggest that NO_2^-
 642 reduction results in an KIE, which should influence the isotopic composition of NO . N_2O here is an intermediate, the isotopic
 643 composition of which is mainly influenced by an EIE between NO and N_2O . The low N_2O yields as well as the N_2O isotopic results
 644 (bulk, SP) clearly suggests that N_2 is produced abiotically.

- Formatiert: Durchgestrichen
- Kommentiert [ML7]: This does not really help and improve things...it is not clear what you want to say here.
- Kommentiert [ML8]: We do not need this to make the point
- Formatiert: Durchgestrichen
- Kommentiert [AV9]: Corrected (colours were missing for some of the bonds)

646 5. Conclusions and outlook

647 In the absence of any clear (genetic) evidence for enzymatic NDFeO from cultures (e.g. *Acidovorax* sp. strain BoFeN1),
648 heterotrophic denitrification/NO₃⁻ reduction coupled to abiotic oxidation of Fe(II) with the NO₂⁻ has been presented as the most
649 reasonable explanation for NDFeO. Here we investigated the second, abiotic step, clearly demonstrating that Fe-associated
650 abiotic NO₂⁻ reduction can be catalysed by mineral and organic phases under environmentally relevant conditions, as found
651 for example in soils and aquifers. Our results confirm that reactive surfaces play a major role with regards to the reaction
652 between NO₂⁻ and Fe(II) and that surface-catalysed chemodenitrification appears to not only contribute to the production of
653 the greenhouse gas N₂O in environments hosting active cycling of Fe and N, but also to an abiotic production of N₂. In order
654 to understand the mechanistic details of Fe-coupled chemodenitrification, natural-abundance measurements of reactive-N
655 isotope ratios may help distinguish between abiotic and biotic reactions during NDFeO. Our results, however, indicate that the
656 potential of coupled N and O isotope measurements to determine the relative importance of Fe-induced N-transformations in
657 natural environments is somewhat limited. Considering, for example, the apparent inverse N isotope effect in the mineral-only
658 experiments, our studies show that the NO₂⁻ N vs. O isotope systematics seem to contrast distinctly between biotic and abiotic
659 NO₂⁻ reduction, potentially permitting the disentanglement of the biotic versus abiotic processes. N₂O SP values seem to be
660 less diagnostic with regards to discriminating between chemodenitrification-derived N₂O and N₂O that is produced during
661 microbial NO₂⁻ reduction. Our results suggest that both the reaction between Fe(II) and reactive N species, as well as the
662 resulting isotope effects, are dependent on the reactive surfaces available. The presence of organic material seems to enhance
663 NO₂⁻ reduction and, to a lesser extent also N₂O production, leading to the enrichment in ¹⁵N in the residual NO₂⁻, as predicted
664 by Rayleigh-type kinetic N isotope fractionation. In the presence of only Fe(II) minerals, NO₂⁻ reduction rates are significantly
665 lower, and net N and O isotope effects are not governed by kinetic isotope fractionation only, but also by isotope equilibrium
666 fractionation during exchange with the ambient mineral phase and/or the ambient water (in the case of O isotopes). While N₂O
667 production was significant, the N₂O yields were below 5%, suggesting that a significant fraction of the NO₂⁻ reduced is at least
668 transiently transformed to NO and possibly N₂. This transient pool of NO possibly stands in quasi-equilibrium with other
669 intermediates (i.e. HNO, NO₂(g)) or complexes (i.e. Fe-NO), and may thereby impact the overall reaction kinetics as well.

670 We speculate that the transient accumulation of NO represents an important constraint both on overall reaction kinetics as well
671 as on the N₂O isotopic signature (or Δ¹⁵N), an aspect that should be verified in future work. Such work may include the
672 quantification of N₂ (and its N isotopic composition), which will help to assess to what extent (i) Fe-mineral surface-induced
673 chemodenitrification leads to the formation of a transient pool of NO and is driven by the catalytically induced abiotic reaction
674 between Fe(II) and NO₂⁻, or if (ii) NO is actually the main oxidizing agent of Fe(II).

675 Our data revealed further complexity with regards to N and O isotope effects during Fe-coupled chemodenitrification than
676 previously reported. We argue that its isotopic imprint depends on the substrate concentration, the presence of reactive surfaces

677 or other catalysts, the mechanisms induced by these catalysts (e.g. surface complexation), and putatively on the intermediates
678 as well as on the product present at the end of the experiments. The multifaceted control on coupled N and O isotope
679 systematics in reactive N species may explain the discrepancies observed between our and previous work (e.g.: with regards
680 to $^{15}\text{E}:$ ^{18}E ratios; Grabb et al. 2017). Clearly, one has to be realistic with regards to using NO_2^- and/or N_2O and O isotope
681 measurements to provide constraints on the relative importance of chemodenitrification under natural conditions. Yet, at this
682 point, there is only a very limited number of studies on the isotope effects of chemodenitrification, and with the results
683 presented here, we expand the body of work that aims at using stable isotope measurements to assess the occurrence of
684 chemodenitrification in denitrifying environments. More work on the controls of stable isotope systematics of
685 chemodenitrification, in particular on the role of reactive, and potentially cryptic, intermediate N species, and of O isotope
686 exchange, will improve our ability to more quantitatively trace Fe-coupled nitrite reduction and N_2O production in natural Fe-
687 rich soil or sedimentary environments.

688 **Data availability**

689 Data can be accessed upon request to the corresponding author.

690 **Author contributions**

691 AAK initiated the project. MFL and AAK supervised the project. ANV designed and conducted all experiments. Isotope
692 measurements as well as data analysis were performed by ANV under the supervision of MFL. JMB conducted Mössbauer
693 measurements and data analysis. PAN supervised and performed all N_2O concentration determination measurements. ANV,
694 SDW and MFL interpreted the data and prepared the paper with inputs from all other co-authors.

695 **Competing interests**

696 The authors declare that they have no conflict of interest.

697 **Acknowledgements**

698 Special thanks go to Karen L. Casciotti (Stanford University) for helping with the correction of the N_2O isotope data. Thanks
699 to Cindy-Louise Lockwood and Toby Samuels for corrections and comments on earlier-versions of the manuscript, and to
700 Viola Warter, Elizabeth Tomaszewski for fruitful discussions on abiotic chemistry and mineral reactions. Markus Maisch is
701 thanked for his help with the preparation of the Mössbauer samples and –Louis Rees for his help with cultivating *S. oneidensis*
702 MR-1.

Formatiert: Schriftart: Kursiv

703 **Funding**

704 This research was supported by the Deutsche Forschungsgemeinschaft - DFG (Grants GRK 1708 Molecular principles of
705 bacterial survival strategies), and through funds from the University of Basel, Switzerland.

706 **References**

- 707 Anderson, I. C. and Levine, J. S.: Relative Rates of Nitric Oxide and Nitrous Oxide Production by Nitrifiers, Denitrifiers, and
708 Nitrate Respirers, *Appl. Environ. Microbiol.*, 51(5), 938–945 [online] Available from:
709 <http://www.ncbi.nlm.nih.gov/pmc/articles/PMC238991/>, 1986.
- 710 Andrews, S. C., Robinson, A. K., Rodriguez-Quinones, F. and Rodríguez-Quinones, F.: Bacterial iron homeostasis, *Fems*
711 *Microbiol. Rev.*, 27(2–3), 215–237, doi:10.1016/s0168-6445(03)00055-x, 2003.
- 712 Baumgärtner, M. and Conrad, R.: Role of nitrate and nitrite for production and consumption of nitric oxide during
713 denitrification in soil, *Fems Microbiol. Lett.*, 101(1), 59–65, doi:10.1111/j.1574-6968.1992.tb05762.x, 1992.
- 714 Braun, V. and Hantke, K.: *The Tricky Ways Bacteria Cope with Iron Limitation*, pp. 31–66, Springer, Dordrecht., 2013.
- 715 Buchwald, C. and Casciotti, K. L.: Isotopic ratios of nitrite as tracers of the sources and age of oceanic nitrite, *Nat. Geosci.*,
716 6(4), 308–313, doi:10.1038/ngeo1745, 2013.
- 717 Buchwald, C., Grabb, K., Hansel, C. M. and Wankel, S. D.: Constraining the role of iron in environmental nitrogen
718 transformations: Dual stable isotope systematics of abiotic NO₂- reduction by Fe(II) and its production of N₂O, *Geochim.*
719 *Cosmochim. Acta*, 186, 1–12, doi:<http://dx.doi.org/10.1016/j.gca.2016.04.041>, 2016.
- 720 Casciotti, K. L.: Inverse kinetic isotope fractionation during bacterial nitrite oxidation, *Geochim. Cosmochim. Acta*, 73(7),
721 2061–2076, doi:10.1016/j.gca.2008.12.022, 2009.
- 722 Casciotti, K. L. and McIlvin, M. R.: Isotopic analyses of nitrate and nitrite from reference mixtures and application to Eastern
723 Tropical North Pacific waters, *Mar. Chem.*, 107(2), 184–201, doi:10.1016/j.marchem.2007.06.021, 2007.
- 724 Casciotti, K. L., Boehlke, J. K., McIlvin, M. R., Mroczkowski, S. J., Hannon, J. E., Böhlke, J. K., McIlvin, M. R.,
725 Mroczkowski, S. J. and Hannon, J. E.: Oxygen isotopes in nitrite: Analysis, calibration, and equilibration, *Anal. Chem.*, 79(6),
726 2427–2436, doi:10.1021/ac061598h, 2007.
- 727 Casciotti, K. L., Buchwald, C., Santoro, A. E. and Frame, C.: Assessment of nitrogen and oxygen isotopic fractionation during
728 nitrification and its expression in the marine environment, in *Methods in Enzymology*, vol. 486, edited by M. G. Klotz, pp.
729 253–280, Academic Press Inc., 2011.
- 730 Chakraborty, A., Roden, E. E., Schieber, J. and Picardal, F.: Enhanced growth of *Acidovorax* sp. strain 2AN during nitrate-
731 dependent Fe(II) oxidation in batch and continuous-flow systems., *Appl. Environ. Microbiol.*, 77(24), 8548–56,
732 doi:10.1128/AEM.06214-11, 2011.
- 733 Charlet, L., Wersin, P. and Stumm, W.: Surface charge of MnCO₃ and FeCO₃, *Geochim. Cosmochim. Acta*, 54(8), 2329–
734 2336, doi:10.1016/0016-7037(90)90059-T, 1990.

735 Chen, D., Liu, T., Li, X., Li, F., Luo, X., Wu, Y. and Wang, Y.: Biological and chemical processes of microbially mediated
736 nitrate-reducing Fe(II) oxidation by *Pseudogulbenkiania* sp. strain 2002, *Chem. Geol.*, 476, 59–69,
737 doi:10.1016/j.chemgeo.2017.11.004, 2018.

738 Choi, P. S., Naal, Z., Moore, C., Casado-Rivera, E., Abruna, H. D., Helmann, J. D. and Shapleigh, J. P.: Assessing the Impact
739 of Denitrifier-Produced NO on other bacteria, *Appl. Environ. Microbiol.*, 72(3), 2200–2205, doi:10.1128/aem.72.3.2200-
740 2205.2006, 2006.

741 Van Cleemput, O. and Samater, A.: Nitrite in soils: accumulation and role in the formation of gaseous N compounds, *Fertil.*
742 *Res.*, 45(1), 81–89, doi:10.1007/BF00749884, 1995.

743 Coby, A. J. and Picardal, F. W.: Inhibition of NO₃- and NO₂- reduction by microbial Fe(III) reduction: Evidence of a reaction
744 between NO₂- and cell surface-bound Fe²⁺, *Appl. Environ. Microbiol.*, 71(9), 5267–5274, doi:10.1128/aem.71.9.5267-
745 5274.2005, 2005.

746 Cornell, R. M. and Schwertmann, U.: *The Iron Oxides: Structure, Properties, Reactions, Occurrences and Uses*, 2nd ed., Wiley-
747 VCH., 2003.

748 Dai, Y.-F., Xiao, Y., Zhang, E.-H., Liu, L.-D., Qiu, L., You, L.-X., Dummi Mahadevan, G., Chen, B.-L. and Zhao, F.: Effective
749 methods for extracting extracellular polymeric substances from *Shewanella oneidensis* MR-1, *Water Sci. Technol.*, 74(12),
750 2987–2996, doi:10.2166/wst.2016.473, 2016.

751 Delahay, P., Pourbaix, M. and Rysselberghe, P. Van: POTENTIAL-pH DIAGRAMS', *J. Chem. Educ.* [online] Available
752 from: <https://pubs.acs.org/doi/pdfplus/10.1021/ed027p683> (Accessed 20 April 2018), 1950.

753 Dhakal, P.: Abiotic nitrate and nitrite reactivity with iron oxide minerals, University of Kentucky., 2013.

754 Dhakal, P., Matocha, C. J., Huggins, F. E. and Vandivere, M. M.: Nitrite Reactivity with Magnetite, *Environ. Sci. Technol.*,
755 47(12), 6206–6213, doi:10.1021/es304011w, 2013.

756 Doane, T. A.: The Abiotic Nitrogen Cycle, *ACS Earth Sp. Chem.*, 1(7), 411–421, doi:10.1021/acsearthspacechem.7b00059,
757 2017.

758 Elsner, M.: Stable isotope fractionation to investigate natural transformation mechanisms of organic contaminants: principles,
759 prospects and limitations, *J. Environ. Monit.*, 12(11), 2005–2031, doi:10.1039/c0em00277a, 2010.

760 Elsner, M., Schwarzenbach, R. P. and Haderlein, S. B.: Reactivity of Fe(II)-Bearing Minerals toward Reductive
761 Transformation of Organic Contaminants, *Environ. Sci. Technol.*, 38(3), 799–807, doi:10.1021/es0345569, 2004.

762 Expert, D.: Iron, an Element Essential to Life, in *Molecular Aspects of Iron Metabolism in Pathogenic and Symbiotic Plant-
763 Microbe Associations*, pp. 1–6, Springer, Dordrecht., 2012.

764 Fowle, D. A. and Konhauser, K. O.: *Microbial Surface Reactivity*, pp. 614–616, Springer, Dordrecht., 2011.

765 Frame, C. H. and Casciotti, K. L.: Biogeochemical controls and isotopic signatures of nitrous oxide production by a marine
766 ammonia-oxidizing bacterium, *Biogeosciences*, 7(9), 2695–2709, doi:10.5194/bg-7-2695-2010, 2010.

767 Fry, B.: *Stable Isotope Ecology*, 3rd ed., Springer Science+Business Media, LLC, New York., 2006.

768 Goretski, J. and Hollocher, T. C.: Trapping of nitric oxide produced during denitrification by extracellular hemoglobin, *J. Biol.*

769 Chem., 263(5), 2316–2323 [online] Available from: <http://www.jbc.org/content/263/5/2316.abstract>, 1988.

770 Gorski, C. A. and Scherer, M. M.: Fe²⁺ sorption at the Fe oxide-water interface: A revised conceptual framework, in *Aquatic*
771 *Redox Chemistry*, vol. 1071, edited by P. G. Tratnyek, T. J. Grundl, and S. B. Haderlein, pp. 315–343, ACS Publications.,
772 2011.

773 Grabb, K. C., Buchwald, C., Hansel, C. M. and Wankel, S. D.: A dual nitrite isotopic investigation of chemodenitrification by
774 mineral-associated Fe(II) and its production of nitrous oxide, *Geochim. Cosmochim. Acta*, 196, 388–402 [online] Available
775 from: <https://www.sciencedirect.com/science/article/pii/S0016703716306044> (Accessed 28 March 2019), 2017.

776 Granger, J. and Sigman, D. M.: Removal of nitrite with sulfamic acid for nitrate N and O isotope analysis with the denitrifier
777 method, *Rapid Commun. Mass Spectrom.*, 23(23), 3753–3762, doi:10.1002/rcm.4307, 2009.

778 Granger, J., Sigman, D. M., Lehmann, M. F. and Tortell, P. D.: Nitrogen and oxygen isotope fractionation during dissimilatory
779 nitrate reduction by denitrifying bacteria, *Limnol. Oceanogr.*, 53(6), 2533–2545, doi:10.4319/lo.2008.53.6.2533, 2008.

780 Granger, J., Karsh, K. L., Guo, W., Sigman, D. M. and Kritee, K.: The nitrogen and oxygen isotope composition of nitrate in
781 the environment: The systematics of biological nitrate reduction, *Geochim. Cosmochim. Acta*, 73(13), A460–A460, 2009.

782 Halder, S., Yadav, K. K., Sarkar, R., Mukherjee, S., Saha, P., Haldar, S., Karmakar, S. and Sen, T.: Alteration of Zeta potential
783 and membrane permeability in bacteria: a study with cationic agents., *Springerplus*, 4, 672, doi:10.1186/s40064-015-1476-7,
784 2015.

785 He, H., Zhang, S., Zhu, C. and Liu, Y.: Equilibrium and kinetic Si isotope fractionation factors and their implications for Si
786 isotope distributions in the Earth's surface environments, *Acta Geochim.*, 35(1), 15–24, doi:10.1007/s11631-015-0079-x,
787 2016a.

788 He, S., Tominski, C., Kappler, A. A., Behrens, S. and Roden, E. E.: Metagenomic analyses of the autotrophic Fe(II)-oxidizing,
789 nitrate-reducing enrichment culture KS, *Appl. Environ. Microbiol.*, 82(9), 2656–2668, doi:10.1128/AEM.03493-15, 2016b.

790 Heidelberg, J. F., Paulsen, I. T., Nelson, K. E., Gaidos, E. J., Nelson, W. C., Read, T. D., Eisen, J. A., Seshadri, R., Ward, N.,
791 Methe, B., Clayton, R. A., Meyer, T., Tsapin, A., Scott, J., Beanan, M., Brinkac, L., Daugherty, S., DeBoy, R. T., Dodson, R.
792 J., Durkin, A. S., Haft, D. H., Kolonay, J. F., Madupu, R., Peterson, J. D., Umayam, L. A., White, O., Wolf, A. M., Vamathevan,
793 J., Weidman, J., Impraim, M., Lee, K., Berry, K., Lee, C., Mueller, J., Khouri, H., Gill, J., Utterback, T. R., McDonald, L. A.,
794 Feldblyum, T. V., Smith, H. O., Venter, J. C., Neilson, K. H. and Fraser, C. M.: Genome sequence of the dissimilatory metal
795 ion-reducing bacterium *Shewanella oneidensis*, *Nat. Biotechnol.*, 20(11), 1118–1123, doi:10.1038/nbt749, 2002.

796 Heil, J., Vereecken, H. and Brüggemann, N.: A review of chemical reactions of nitrification intermediates and their role in
797 nitrogen cycling and nitrogen trace gas formation in soil, *Eur. J. Soil Sci.*, 67(1), 23–39, doi:10.1111/ejss.12306, 2016.

798 Hunkeler, D. and Elsner, M.: Principles and Mechanisms of Isotope Fractionation, in *Environmental Isotopes in*
799 *Biodegradation and Bioremediation*, edited by M. Aelion Höhener, P., Hunkeler, D., pp. 43–76, CRC Press., 2009.

800 Ilbert, M. and Bonnefoy, V.: Insight into the evolution of the iron oxidation pathways, *Biochim. Biophys. Acta - Bioenerg.*,
801 1827(2), 161–175, doi:<http://dx.doi.org/10.1016/j.bbabbio.2012.10.001>, 2013.

802 Jamieson, J., Prommer, H., Kaksonen, A. H., Sun, J., Siade, A. J., Yusov, A. and Bostick, B.: Identifying and Quantifying the

803 Intermediate Processes during Nitrate-Dependent Iron(II) Oxidation, Environ. Sci. Technol., acs.est.8b01122,
804 doi:10.1021/acs.est.8b01122, 2018.

805 Jones, L. C., Peters, B., Lezama Pacheco, J. S., Casciotti, K. L. and Fendorf, S.: Stable Isotopes and Iron Oxide Mineral
806 Products as Markers of Chemodenitrification, Environ. Sci. Technol., 49(6), 3444–3452, doi:10.1021/es504862x, 2015.

807 Kampschreur, M. J. M. J., Kleerebezem, R., de Vet, W. W. J. M. J. M. and van Loosdrecht, M. C. M. M.: Reduced iron induced
808 nitric oxide and nitrous oxide emission, Water Res., 45(18), 5945–5952, doi:http://dx.doi.org/10.1016/j.watres.2011.08.056,
809 2011.

810 Kendall, C. and Aravena, R.: Nitrate Isotopes in Groundwater Systems, , 261–297, doi:10.1007/978-1-4615-4557-6_9, 2000.

811 Klueglein, N. and Kappler, A. A.: Abiotic oxidation of Fe(II) by reactive nitrogen species in cultures of the nitrate-reducing
812 Fe(II) oxidizer Acidovorax sp BoFeN1 - questioning the existence of enzymatic Fe(II) oxidation, Geobiology, 11(2), 396,
813 doi:10.1111/gbi.12040, 2013.

814 Klueglein, N., Zeitvogel, F., Stierhof, Y.-D., Floetenmeyer, M., Konhauser, K. O., Kappler, A. A. and Obst, M.: Potential Role
815 of Nitrite for Abiotic Fe(II) Oxidation and Cell Encrustation during Nitrate Reduction by Denitrifying Bacteria, Appl. Environ.
816 Microbiol., 80(3), 1051–1061, doi:10.1128/aem.03277-13, 2014.

817 Lagarec, K. and Rancourt, D. G.: Extended Voigt-based analytic lineshape method for determining N-dimensional correlated
818 hyperfine parameter distributions in Mössbauer spectroscopy, Nucl. Instruments Methods Phys. Res. Sect. B Beam Interact.
819 with Mater. Atoms, 129(2), 266–280, doi:10.1016/S0168-583X(97)00284-X, 1997.

820 Laufer, K., Roy, H., Jørgensen, B. B. and Kappler, A. A.: Evidence for the existence of autotrophic nitrate-reducing Fe(II)-
821 oxidizing bacteria in marine coastal sediment, Appl. Environ. Microbiol., 82(20), 6120–6131, doi:10.1128/AEM.01570-16,
822 2016.

823 Li, W., Beard, B. L. and Johnson, C. M.: Exchange and fractionation of Mg isotopes between epsomite and saturated MgSO
824 4 solution, Geochim. Cosmochim. Acta, 75, 1814–1828, doi:10.1016/j.gca.2011.01.023, 2011.

825 Lies, D. P., Hernandez, M. E., Kappler, A. A., Mielke, R. E., Gralnick, J. A. and Newman, D. K.: Shewanella oneidensis MR-
826 1 uses overlapping pathways for iron reduction at a distance and by direct contact under conditions relevant for biofilms, Appl.
827 Environ. Microbiol., 71(8), 4414–4426, doi:10.1128/aem.71.8.4414-4426.2005, 2005.

828 Liu, J. and Konermann, L.: Irreversible Thermal Denaturation of Cytochrome c Studied by Electrospray Mass Spectrometry,
829 J. Am. Soc. Mass Spectrom., 20(5), 819–828, doi:10.1016/J.JASMS.2008.12.016, 2009.

830 Liu, J., Wang, Z., Belchik, S. M., Edwards, M. J., Liu, C., Kennedy, D. W., Merkley, E. D., Lipton, M. S., Butt, J. N.,
831 Richardson, D. J., Zachara, J. M., Fredrickson, J. K., Rosso, K. M. and Shi, L.: Identification and Characterization of MtoA:
832 A Decaheme c-Type Cytochrome of the Neutrophilic Fe(II)-Oxidizing Bacterium Sideroxydans lithotrophicus ES-1., Front.
833 Microbiol., 3, 37, doi:10.3389/fmicb.2012.00037, 2012.

834 Liu, T., Chen, D., Luo, X., Li, X. and Li, F.: Microbially mediated nitrate-reducing Fe(II) oxidation: Quantification of
835 chemodenitrification and biological reactions, Geochim. Cosmochim. Acta, doi:10.1016/J.GCA.2018.06.040, 2018.

836 Lovley, D. R.: Microbial Fe(III) reduction in subsurface environments, FEMS Microbiol. Rev., 20(3–4), 305–313,

837 doi:10.1111/j.1574-6976.1997.tb00316.x, 1997.

838 Lovley, D. R.: Electromicrobiology, *Annu. Rev. Microbiol.*, 66(1), 391–409, doi:10.1146/annurev-micro-092611-150104,

839 2012.

840 Luan, F., Liu, Y., Griffin, A. M., Gorski, C. A. and Burgos, W. D.: Iron(III)-Bearing Clay Minerals Enhance Bioreduction of

841 Nitrobenzene by *Shewanella putrefaciens* CN32, *Env. Sci Technol*, 49, 1418–1476, doi:10.1021/es504149y, 2015.

842 Luna-Zaragoza, D., Romero-Guzmán, E. T. and Reyes-Gutiérrez, L. R.: Surface and Physicochemical Characterization of

843 Phosphates Vivianite,

844 $\text{Fe}_2(\text{PO}_4)_3$ and Hydroxyapatite, $\text{Ca}_5(\text{OH})(\text{PO}_4)_3$, *J. Miner. Mater. Charact. Eng.*,

845 08(08), 591–609, doi:10.4236/jmmce.2009.88052, 2009.

847 Mariotti, A., Germon, J. C., Hubert, P., Kaiser, P., Letolle, R., Tardieux, A. and Tardieux, P.: Experimental-Determination of

848 Nitrogen Kinetic Isotope Fractionation - Some Principles - Illustration for the Denitrification and Nitrification Processes, *Plant*

849 *Soil*, 62(3), 413–430, doi:10.1007/Bf02374138, 1981.

850 Martin, T. S. and Casciotti, K. L.: Paired N and O isotopic analysis of nitrate and nitrite in the Arabian Sea oxygen deficient

851 zone, *Deep. Res. Part I Oceanogr. Res. Pap.*, 121, 121–131, doi:10.1016/j.dsr.2017.01.002, 2017.

852 McIlvin, M. R. and Altabet, M. A.: Chemical conversion of nitrate and nitrite to nitrous oxide for nitrogen and oxygen isotopic

853 analysis in freshwater and seawater, *Anal. Chem.*, 77(17), 5589–5595, doi:10.1021/ac050528s, 2005.

854 McIlvin, M. R. and Casciotti, K. L.: Fully automated system for stable isotopic analyses of dissolved nitrous oxide at natural

855 abundance levels, *Limnol. Oceanogr. Methods*, 8(2), 54–66, doi:10.4319/lom.2010.8.54, 2010.

856 McKnight, G. M., Smith, L. M., Drummond, R. S., Duncan, C. W., Golden, M. and Benjamin, N.: Chemical synthesis of nitric

857 oxide in the stomach from dietary nitrate in humans., *Gut*, 40(2), 211–4 [online] Available from:

858 <http://www.ncbi.nlm.nih.gov/pubmed/9071933> (Accessed 18 March 2018), 1997.

859 Minguzzi, A., Fan, F.-R. F., Vertova, A., Rondinini, S. and Bard, A. J.: Dynamic potential–pH diagrams application to

860 electrocatalysts for wateroxidation, *Chem. Sci.*, 3(1), 217–229, doi:10.1039/C1SC00516B, 2012.

861 Miot, J., Remusat, L., Duprat, E., Gonzalez, A., Pont, S. and Poinso, M. M.: Fe biomineralization mirrors individual metabolic

862 activity in a nitrate-dependent Fe(II)-oxidizer, *Front. Microbiol.*, 6(SEP), 879, doi:10.3389/fmicb.2015.00879, 2015.

863 Mohn, J., Wolf, B., Toyoda, S., Lin, C.-T., Liang, M.-C., Brüggemann, N., Wissel, H., Steiker, A. E., Dyckmans, J., Szwee,

864 L., Ostrom, N. E., Casciotti, K. L., Forbes, M., Giesemann, A., Well, R., Doucett, R. R., Yarnes, C. T., Ridley, A. R., Kaiser,

865 J. and Yoshida, N.: Interlaboratory assessment of nitrous oxide isotopomer analysis by isotope ratio mass spectrometry and

866 laser spectroscopy: current status and perspectives, *Rapid Commun. Mass Spectrom.*, 28(18), 1995–2007,

867 doi:10.1002/rcm.6982, 2014.

868 Muehe, E. M., Gerhardt, S., Schink, B. and Kappler, A.: Ecophysiology and the energetic benefit of mixotrophic Fe(II)

869 oxidation by various strains of nitrate-reducing bacteria, *FEMS Microbiol. Ecol.*, 70(3), 335–343, doi:10.1111/j.1574-

870 6941.2009.00755.x, 2009.

871 Muehe, E. M., Obst, M., Hitchcock, A., Tylliszczak, T., Behrens, S., Schröder, C., Byrne, J. M., Michel, F. M., Krämer, U. and
872 Kappler, A. A.: Fate of Cd during microbial Fe(III) mineral reduction by a novel and Cd-tolerant geobacter species, *Environ.*
873 *Sci. Technol.*, 47(24), 14099–14109, doi:10.1021/es403365w, 2013.

874 Nelson, D. W. and Bremner, J. M.: Factors affecting chemical transformations of nitrite in soils, *Soil Biol. Biochem.*, 1(3),
875 229–239, doi:10.1016/0038-0717(69)90023-6, 1969.

876 Niklaus, P. A., Le Roux, X., Poly, F., Buchmann, N., Scherer-Lorenzen, M., Weigelt, A. and Barnard, R. L.: Plant species
877 diversity affects soil–atmosphere fluxes of methane and nitrous oxide, *Oecologia*, 181(3), 919–930, doi:10.1007/s00442-016-
878 3611-8, 2016.

879 Nordhoff, M., Tominski, C., Halama, M., Byrne, J. M., Obst, M., Kleindienst, S., Behrens, S. and Kappler, A. A.: Insights into
880 nitrate-reducing Fe(II) oxidation mechanisms through analysis of cell-mineral associations, cell encrustation, and mineralogy
881 in the chemolithoautotrophic enrichment culture KS, *Appl. Environ. Microbiol.*, 83(13), e00752-17, doi:10.1128/AEM.00752-
882 17, 2017.

883 Ostrom, N. E. and Ostrom, P.: *Handbook of Environmental Isotope Geochemistry*, 1st ed., edited by M. Baskaran, Springer
884 Berlin Heidelberg, Berlin, Heidelberg., 2011.

885 Ostrom, N. E. and Ostrom, P. H.: The Isotopomers of Nitrous Oxide: Analytical Considerations and Application to Resolution
886 of Microbial Production Pathways, in *Handbook of Environmental Isotope Geochemistry: Vol I*, edited by M. Baskaran, pp.
887 453–476, Springer Berlin Heidelberg, Berlin, Heidelberg., 2012.

888 Ostrom, N. E., Pitt, A., Sutka, R., Ostrom, P. H., Grandy, A. S., Huizinga, K. M. and Robertson, G. P.: Isotopologue effects
889 during N₂O reduction in soils and in pure cultures of denitrifiers, *J. Geophys. Res.*, 112(G2), doi:10.1029/2006jg000287, 2007.

890 Ostrom, N. E., Gandhi, H., Coplen, T. B., Toyoda, S., Böhlke, J. K., Brand, W. A., Casciotti, K. L., Dyckmans, J., Giesemann,
891 A., Mohn, J., Well, R., Yu, L. and Yoshida, N.: Preliminary assessment of stable nitrogen and oxygen isotopic composition of
892 USGS51 and USGS52 nitrous oxide reference gases and perspectives on calibration needs, *Rapid Commun. Mass Spectrom.*,
893 32(15), 1207–1214, doi:10.1002/rcm.8157, 2018.

894 Otte, J. M., Blackwell, N., Ruser, R., Kappler, A. A., Kleindienst, S. and Schmidt, C.: N₂O formation by nitrite-induced
895 (chemo)denitrification in coastal marine sediment, *Sci. Rep.*, 9(1), 10691, doi:10.1038/s41598-019-47172-x, 2019.

896 Ottley, C. J., Davison, W. and Edmunds, W. M.: Chemical catalysis of nitrate reduction by iron(II), *Geochim. Cosmochim.*
897 *Acta*, 61(9), 1819–1828, doi:Doi 10.1016/S0016-7037(97)00058-6, 1997.

898 Pereira, C., Ferreira, N. R., Rocha, B. S., Barbosa, R. M. and Laranjinha, J.: The redox interplay between nitrite and nitric
899 oxide: From the gut to the brain, *Redox Biol.*, 1(1), 276–284, doi:http://dx.doi.org/10.1016/j.redox.2013.04.004, 2013.

900 Phillips, R. L., Song, B., McMillan, A. M. S., Grelet, G., Weir, B. S., Palmada, T. and Tobias, C.: Chemical formation of
901 hybrid di-nitrogen calls fungal codenitrification into question, *Sci. Rep.*, 6(1), 39077, doi:10.1038/srep39077, 2016.

902 Piasecki, W., Szymanek, K. and Charmas, R.: Fe²⁺ adsorption on iron oxide: the importance of the redox potential of the
903 adsorption system, *Adsorption*, doi:10.1007/s10450-019-00054-0, 2019.

904 Piepenbrock, A., Dippon, U., Porsch, K., Appel, E. and Kappler, A. A.: Dependence of microbial magnetite formation on

905 humic substance and ferrihydrite concentrations, *Geochim. Cosmochim. Acta*, 75(22), 6844–6858,
906 doi:10.1016/j.gca.2011.09.007, 2011.

907 Price, A., Macey, M. C., Miot, J. and Olsson-Francis, K.: Draft Genome Sequences of the Nitrate-Dependent Iron-Oxidizing
908 Proteobacteria *Acidovorax* sp. Strain BoFeN1 and *Paracoccus pantotrophus* Strain KS1, edited by J. C. Thrash, *Microbiol.*
909 *Resour. Announc.*, 7(10), e01050-18, doi:10.1128/mra.01050-18, 2018.

910 Rakshit, S., Matocha, C. J. and Coyne, M. S.: Nitrite reduction by siderite, *Soil Sci. Soc. Am. J.*, 72(4), 1070–1077,
911 doi:10.2136/sssaj2007.0296, 2008.

912 Rancourt, D. G. and Ping, J. Y.: Voigt-based methods for arbitrary-shape static hyperfine parameter distributions in Mössbauer
913 spectroscopy, *Nucl. Instruments Methods Phys. Res. Sect. B Beam Interact. with Mater. Atoms*, 58(1), 85–97,
914 doi:10.1016/0168-583X(91)95681-3, 1991.

915 Rivallan, M., Ricchiardi, G., Bordiga, S. and Zecchina, A.: Adsorption and reactivity of nitrogen oxides (NO₂, NO, N₂O) on
916 Fe-zeolites, *J. Catal.*, 264(2), 104–116, doi:10.1016/j.jcat.2009.03.012, 2009.

917 Samarkin, V. A., Madigan, M. T., Bowles, M. W., Casciotti, K. L., Priscu, J. C., McKay, C. P. and Joye, S. B.: Abiotic nitrous
918 oxide emission from the hypersaline Don Juan Pond in Antarctica, *Nat. Geosci.*, 3(5), 341–344, doi:10.1038/ngeo847, 2010.

919 Schaefer, M. V.: Spectroscopic evidence for interfacial Fe(II)- Fe(III) electron transfer in clay minerals, *Iowa Research Online*.
920 [online] Available from: <http://ir.uiowa.edu/etd/596> (Accessed 20 March 2018), 2010.

921 Sigman, D. M., DiFiore, P. J., Hain, M. P., Deutsch, C., Wang, Y., Karl, D. M., Knapp, A. N., Lehmann, M. F. and Pantoja,
922 S.: The dual isotopes of deep nitrate as a constraint on the cycle and budget of oceanic fixed nitrogen, *Deep. Res. Part I-*
923 *Oceanographic Res. Pap.*, 56(9), 1419–1439, doi:10.1016/j.dsr.2009.04.007, 2009.

924 Snyder, L. R. and Adler, H. J.: Dispersion in Segmented Flow through Glass Tubing in Continuous-Flow Analysis: The Ideal
925 Model, *Anal. Chem.*, 48(7), 1017–1022, doi:10.1021/ac60371a013, 1976.

926 Sorensen, J. and Thorling, L.: Stimulation by Lepidocrocite (Gamma-Fe₂O₃) of Fe(II)-Dependent Nitrite Reduction, *Geochim.*
927 *Cosmochim. Acta*, 55(5), 1289–1294, doi:10.1016/0016-7037(91)90307-Q, 1991.

928 Stevenson, F. J., Harrison, R. M., Wetselaar, R. and Leeper, R. A.: Nitrosation of Soil Organic Matter: III. Nature of Gases
929 Produced by Reaction of Nitrite with Lignins, Humic Substances, and Phenolic Constituents Under Neutral and Slightly Acidic
930 Conditions I, *Soil Sci. Soc. Am. J.*, 34(3), 430, doi:10.2136/sssaj1970.03615995003400030024x, 1970.

931 Stookey, L. L.: FERROZINE - A NEW SPECTROPHOTOMETRIC REAGENT FOR IRON, *Anal. Chem.*, 42(7), 779-
932 doi:10.1021/ac60289a016, 1970.

933 Straub, K. L., Benz, M., Schink, B. and Widdel, F.: Anaerobic, nitrate-dependent microbial oxidation of ferrous iron, *Appl.*
934 *Environ. Microbiol.*, 62(4), 1458–1460, 1996.

935 Stumm, W. and Sulzberger, B.: The cycling of iron in natural environments: Considerations based on laboratory studies of
936 heterogeneous redox processes, *Geochim. Cosmochim. Acta*, 56(8), 3233–3257, doi:10.1016/0016-7037(92)90301-X, 1992.

937 Sutka, R. L., Ostrom, N. E., Ostrom, P. H., Breznak, J. A., Gandhi, H., Pitt, A. J. and Li, F.: Distinguishing nitrous oxide
938 production from nitrification and denitrification on the basis of isotopomer abundances, *Appl. Environ. Microbiol.*, 72(1),

939 638–644, doi:10.1128/Aem.72.1.638-644.2006, 2006.

940 Tanford, C.: Protein denaturation: Part c. theoretical models for the mechanism of denaturation, *Adv. Protein Chem.*, 24(C),
941 1–95, doi:10.1016/S0065-3233(08)60241-7, 1970.

942 Taran, Y. A., Kliger, G. A., Cienfuegos, E. and Shuykin, A. N.: Carbon and hydrogen isotopic compositions of products of
943 open-system catalytic hydrogenation of CO₂: Implications for abiogenic hydrocarbons in Earth's crust, *Geochim. Cosmochim.*
944 *Acta*, 74(21), 6112–6125, doi:10.1016/j.gca.2010.08.012, 2010.

945 Tian, T., Zhou, K., Xuan, L., Zhang, J.-X., Li, Y.-S., Liu, D.-F. and Yu, H.-Q.: Exclusive microbially driven autotrophic iron-
946 dependent denitrification in a reactor inoculated with activated sludge, *Water Res.*, 170, 115300,
947 doi:10.1016/j.watres.2019.115300, 2020.

948 Tiso, M. and Schechter, A. N.: Nitrate reduction to nitrite, nitric oxide and ammonia by gut bacteria under physiological
949 conditions., *PLoS One*, 10(3), e0119712, doi:10.1371/journal.pone.0119712, 2015.

950 Tominski, C., Heyer, H., Lösekann-Behrens, T., Behrens, S. and Kappler, A. A.: Growth and Population Dynamics of the
951 Anaerobic Fe(II)-Oxidizing and Nitrate-Reducing Enrichment Culture KS, edited by F. E. Löffler, *Appl. Environ. Microbiol.*,
952 84(9), e02173-17, doi:10.1128/AEM.02173-17, 2018.

953 Toyoda, S. and Yoshida, N.: Determination of Nitrogen Isotopomers of Nitrous Oxide on a Modified Isotope Ratio Mass
954 Spectrometer, , doi:10.1021/AC9904563, 1999.

955 Toyoda, S., Mutoke, H., Yamagishi, H., Yoshida, N. and Tanji, Y.: Fractionation of N₂O isotopomers during production by
956 denitrifier, *Soil Biol. Biochem.*, 37(8), 1535–1545, doi:10.1016/j.soilbio.2005.01.009, 2005.

957 Veeramani, H., Alessi, D. S., Suvorova, E. I., Lezama-Pacheco, J. S., Stubbs, J. E., Sharp, J. O., Dippon, U., Kappler, A. A.,
958 Bargar, J. R. and Bernier-Latmani, R.: Products of abiotic U(VI) reduction by biogenic magnetite and vivianite, *Geochim.*
959 *Cosmochim. Acta*, 75(9), 2512–2528, doi:10.1016/j.gca.2011.02.024, 2011.

960 Wankel, S. D., Ziebis, W., Buchwald, C., Charoenpong, C., De Beer, Di., Dentinger, J., Xu, Z. and Zengler, K.: Evidence for
961 fungal and chemodenitrification based N₂O flux from nitrogen impacted coastal sediments, *Nat. Commun.*, 8(1), 15595,
962 doi:10.1038/ncomms15595, 2017.

963 Weber, K. A., Hedrick, D. B., Peacock, A. D., Thrash, J. C., White, D. C., Achenbach, L. A. and Coates, J. D.: Physiological
964 and taxonomic description of the novel autotrophic, metal oxidizing bacterium, *Pseudogulbenkiania* sp strain 2002, *Appl.*
965 *Microbiol. Biotechnol.*, 83(3), 555–565, doi:10.1007/s00253-009-1934-7, 2009.

966 Well, R. and Flessa, H.: Isotopologue signatures of N₂O produced by denitrification in soils, *J. Geophys. Res.*, 114,
967 doi:10.1029/2008jg000804, 2009.

968 Wenk, C. B., Frame, C. H., Koba, K., Casciotti, K. L., Veronesi, M., Niemann, H., Schubert, C. J., Yoshida, N., Toyoda, S.,
969 Makabe, A., Zopfi, J. and Lehmann, M. F.: Differential N₂O dynamics in two oxygen-deficient lake basins revealed by stable
970 isotope and isotopomer distributions, *Limnol. Oceanogr.*, 61(5), 1735–1749, doi:10.1002/lno.10329, 2016.

971 White, G. F., Edwards, M. J., Gomez-Perez, L., Richardson, D. J., Butt, J. N. and Clarke, T. A.: Mechanisms of Bacterial
972 Extracellular Electron Exchange, in *Advances in Microbial Physiology*, vol. 68, pp. 87–138., 2016.

973 Widdel, F. and Pfennig, N.: STUDIES ON DISSIMILATORY SULFATE-REDUCING BACTERIA THAT DECOMPOSE
974 FATTY-ACIDS .1. ISOLATION OF NEW SULFATE-REDUCING BACTERIA ENRICHED WITH ACETATE FROM
975 SALINE ENVIRONMENTS - DESCRIPTION OF DESULFOBACTER-POSTGATEI GEN-NOV, SP-NOV, Arch.
976 Microbiol., 129(5), 395–400, doi:10.1007/bf00406470, 1981.

977 Widdel, F., Kohring, G.-W. and Mayer, F.: Studies on Dissimilatory Sulfate-Reducing Bacteria that Decompose Fatty Acids,
978 Arch Microbiol, 134, 286–294 [online] Available from: <https://link.springer.com/content/pdf/10.1007/BF00407804.pdf>
979 (Accessed 22 April 2018), 1983.

980 Wilson, W. W., Wade, M. M., Holman, S. C. and Champlin, F. R.: Status of methods for assessing bacterial cell surface charge
981 properties based on zeta potential measurements, J. Microbiol. Methods, 43(3), 153–164, doi:10.1016/S0167-7012(00)00224-
982 4, 2001.

983 Winther, M., Balslev-Harder, D., Christensen, S., Priemé, A., Elberling, B., Crosson, E. and Blunier, T.: Continuous
984 measurements of nitrous oxide isotopomers during incubation experiments, Biogeosciences, 15(3), 767–780, doi:10.5194/bg-
985 15-767-2018, 2018.

986 Wunderlin, P., Lehmann, M. F., Siegrist, H., Tuzson, B., Joss, A., Emmenegger, L. and Mohn, J.: Isotope Signatures of N₂O
987 in a Mixed Microbial Population System: Constraints on N₂O Producing Pathways in Wastewater Treatment, Environ. Sci.
988 Technol., 130118101927005, doi:10.1021/es303174x, 2013.

989 Ye, R. W., Averill, B. A. and Tiedje, J. M.: Denitrification: production and consumption of nitric oxide, Appl. Environ.
990 Microbiol., 60(4), 1053–1058 [online] Available from: <http://www.ncbi.nlm.nih.gov/pmc/articles/PMC201439/>, 1994.

991 Zeitvogel, F., Burkhardt, C. J., Schroepel, B., Schmid, G., Ingino, P. and Obst, M.: Comparison of Preparation Methods of
992 Bacterial Cell-Mineral Aggregates for SEM Imaging and Analysis Using the Model System of *Acidovorax* sp. BoFeN1,
993 Geomicrobiol. J., 34(4), 317–327, doi:10.1080/01490451.2016.1189467, 2017.

994 Zhu-Barker, X., Cavazos, A. R., Ostrom, N. E., Horwath, W. R. and Glass, J. B.: The importance of abiotic reactions for
995 nitrous oxide production, Biogeochemistry, 126(3), 251–267, doi:10.1007/s10533-015-0166-4, 2015.

996 Zumft, W. G.: Cell biology and molecular basis of denitrification, Microbiol. Mol. Biol. Rev., 61(4), 533–+ [online] Available
997 from: <http://www.ncbi.nlm.nih.gov/pubmed/9409151> (Accessed 19 February 2018), 1997.

998 Zweier, J. L., Samouilov, A. and Kuppasamy, P.: Non-enzymatic nitric oxide synthesis in biological systems, Biochim.
999 Biophys. Acta - Bioenerg., 1411(2–3), 250–262, doi:10.1016/S0005-2728(99)00018-3, 1999.

1000

Kommentiert [ML10]: Check refs...they seem unformatted, some are messed up of only in capital letters (e.g. Widdel)